https://doi.org/10.5194/egusphere-2026-1023
Preprint. Discussion started: 16 March 2026

Unraveling the chemical structures and sources of biomass-derived organic aerosols through a year-long offline analysis in Hyytiälä, Finland

Qianzhe Sun[1], Ruichen Zhou[2], Sho Ohata[2], Chiaki Shirota[3], Tuukka Petäjä[4], Ilona Ylivinkka[4], Lauri Ahonen[4], Markku Kulmala[4] and Michihiro Mochida[1,2]
[1]Graduate School of Environmental Studies, Nagoya University, Nagoya, Japan
[2]Institute for Space-Earth Environmental Research, Nagoya University, Nagoya, Japan
[3]Murata Keisokuki Service Co., Ltd., Yokohama, Japan
[4]Institute for Atmospheric and Earth System Research (INAR)/Physics, University of Helsinki, Helsinki, Finland

Correspondence to: Michihiro Mochida (mochida@isee.nagoya-u.ac.jp)

Abstract

Biomass-burning OA (BBOA) and biogenic secondary OA (BSOA), both originating from biomass but from different pathways, still lack comprehensive and quantitative understanding, which limits assessments of their environmental impacts. In this study, source-resolved OAs including BBOA and BSOA in a European boreal forest were characterized by the offline use of an aerosol mass spectrometer (AMS), with improved chemical resolution offered by polarity-based fractionation. OA extract solutions were prepared according to polarity as high-polarity water-soluble organic matter, humic-like substances, and water-insoluble organic matter, and their abundances and chemical structures were analyzed by off-line high-resolution AMS analysis. Quantitative analysis revealed an annual OA concentration of 1.24 ± 0.75 μg m^{-3}, with lower concentrations in winter and higher in summer. A 5-factor source apportionment solution was obtained from positive matrix factorization (PMF) of the mass spectra of the three fractions. CHN-family ions were found to be indicative of BBOA, whereas $C_5H_8O_5^+$, $C_5H_6O^+$, and $C_8H_9O_4^+$ were identified as potential tracers for BSOA; they lead the identification of BBOA- and BSOA-like factors. CROA factor, related to aged fossil fuel combustion and aged biomass material combustion, was also identified. Different PMF factors exhibited differences in water solubility, with relatively water-insoluble characteristics of compounds containing CROA aromatic structures. This study highlights the usefulness of polarity-resolved factor analysis in understanding diverse OA sources and opens the door for the characterization of climate- and air-quality-related properties of BBOA and BSOA.

1 Introduction

Biomass-burning organic aerosol (BBOA) and biogenic secondary organic aerosol (BSOA) are two types of organic aerosols (OAs) that originate from biomass sources, but have vastly different formation pathways. Biomass burning is among the greatest sources of atmospheric OAs and has become a global environmental concern (Simoneit, 2002; Laskin et al., 2009).

https://doi.org/10.5194/egusphere-2026-1023
Preprint. Discussion started: 16 March 2026

The chemical composition and physicochemical properties of BBOA are highly dependent on the type of biomass burned. For instance, fresh biomass emissions from wildfires differ substantially from those associated with agricultural residues, fallen leaves, or decaying wood (Ma et al., 2024). BSOA originate from the atmospheric oxidation of biogenic volatile organic compounds (BVOCs), whose emission strength and chemical profiles are strongly influenced by vegetation type and meteorological conditions (Qin et al., 2018; Müller et al., 2020). Globally, terrestrial vegetation emits more than 1 Pg of BVOCs annually, making it a dominant source of secondary organic aerosols (Guenther et al., 2012; Zheng et al., 2023). The separate quantification of BBOA and BSOA is required to understand the respective effects of these two types of organic aerosols (OAs) on climate and air quality through their distinct properties. The effect based on their light absorptivity is a representative example to be studied, as BBOA is considered a major source of light-absorbing OA (Li et al., 2025; Afsana et al., 2022), whereas BSOA is regarded as weakly light-absorbing (Deng et al., 2019).

A single, definitive technique for distinguishing between BBOA and BSOA has yet to be established, since most available methods have inherent limitations as well as advantages. For example, radiocarbon (^{14}C) analysis is widely used to distinguish between fossil fuel and modern carbon sources, but it is not effective for differentiating BSOA from BBOA (Dusek et al., 2017; Szidat et al., 2006). The organic carbon (OC)-to-elemental carbon (EC) ratio can be used to estimate the abundance of primary organic carbon (POC) and secondary organic carbon (SOC), but it cannot serve as a robust approach for source apportionment (Gelencsér et al., 2007; Dusek et al., 2017). Molecular-tracer-based methods, which use source-specific molecular markers, are among the most widely applied approaches and enable the quantification of various compound classes (Cheng et al., 2021; Haque et al., 2023; Gilardoni et al., 2011). The chemical mass balance (CMB) model is a source apportionment technique that relies on source profiles and molecular tracer concentrations, but the apportionment of SOAs using CMB remains highly uncertain, partly owing to the atmospheric degradation of organic tracers and the challenges associated with the representativeness of the source profiles used (Yin et al., 2015; Srivastava et al., 2018; Schauer et al., 1996). The combination of aerosol mass spectrometer (AMS) measurements and positive matrix factorization (PMF) has also been widely applied for source apportionment of OAs in online studies (Corrigan et al., 2013; Ulbrich et al., 2009a). As a receptor model, PMF resolves measured mass spectral data into different factors that represent distinct source profiles and their temporal contributions (Zhang et al., 2011). However, distinguishing BBOA and BSOA has generally not been achieved in online AMS studies without additional tools (Liu et al., 2016; Zhang et al., 2024). The above methods are often jointly applied in studies aiming to distinguish between BBOA and BSOA, as each has its own advantages and limitations.

The offline application of high-resolution AMS (HR–AMS) measurement with PMF, which has emerged in recent years (Zhou et al., 2021) , is a possible new approach to advance the source apportionment of OA. Various methods to extract chemical components from aerosol samples collected on filters have been developed for offline AMS analysis, including the use of water (Duarte and Duarte, 2011), ethanol (Cheng et al., 2016), and ethyl acetate (Mihara and Mochida, 2011) as solvents for extraction. Recently, solid-phase extraction (SPE) to isolate fractions with distinct polarities has been applied in offline AMS studies, allowing for a detailed investigation of OA properties with high extraction efficiency (Chen et al., 2016). Humic-like

https://doi.org/10.5194/egusphere-2026-1023
Preprint. Discussion started: 16 March 2026

substances (HULIS) comprise a subset of water-soluble organic matter (WSOM) isolated by using SPE and are named for their resemblance to terrestrial and aquatic humic and fulvic acids (Lin et al., 2010). Compared with HULIS, the remaining water-soluble fraction, high-polarity WSOM (HP-WSOM), is generally considered to have lower light absorptivity and greater hygroscopicity (Lin et al., 2010; Zhang et al., 2022; Gysel et al., 2004). Water-insoluble organic matter (WISOM) consists of relatively high-molecular-weight compounds (Chen et al., 2016) and has strong light absorption (Chen et al., 2017). Previous studies using offline HR–AMS analysis have shown that the polarity of different OA fractions is positively correlated with the O/C ratio and that each fraction is dominated by distinct PMF factors (Zhou et al., 2021). Compared with conventional online AMS analysis, the addition of polarity-based fractionation improves the chemical resolution and may aid in the identification and quantification of OA sources, including BBOA and BSOA.

In conventional AMS studies, various mass spectral ion tracers have been adopted to differentiate between BBOA and BSOA. Compared with the molecular-tracer-based approach, the molecular-level fragmentation inherent to AMS analysis allows the retention of key fragment ions, which potentially makes it a more robust approach for source apportionment because it can incorporate the full range of ion fragments. For example, $C_5H_6O^+$ (m/z 82) has been recognized as a highly specific and quantitative tracer for isoprene-derived SOAs (Hu et al., 2015). In contrast, monoterpene-derived SOAs generally produce nonspecific hydrocarbon fragments such as $C_5H_7^+$, $C_6H_9^+$, and $C_7H_7^+$, and reliable fragment ion tracers have yet to be firmly established. BBOA are typically characterized by the presence of levoglucosan, a cellulose pyrolysis product and tracer for fresh biomass burning emissions (Jolleys et al., 2015). However, its atmospheric lifetime is estimated to be short, for example, 0.7–2.2 days under OH radical exposure (Hennigan et al., 2010), making it difficult to detect in air masses transported over long ranges (Zhang et al., 2024). Moreover, alkyl amides and nitriles have been identified as potential tracers for biomass burning. High temperatures during combustion promote the release of ammonia and amines that react with carboxylic acids to form alkyl amides, which can further undergo dehydration to yield alkyl nitriles (Chen et al., 2018; Ratcliff et al., 1974; Simoneit et al., 2003). As a result, nitrogen-containing organic compounds (NOCs) in biomass burning-derived aerosols contribute to the detection of both CHN and CHON ion groups in AMS analysis (Laskin et al., 2009). In contrast, OAs from biogenic volatile organic compounds (BVOCs), including α-pinene and limonene, primarily generate CHON ions instead of CHN ions through oxidation and nitration processes, as detected by AMS (Laskin et al., 2014). Therefore, CHN family ions detected by AMS may serve as novel tracers for BBOA. The fragment ions obtained via AMS described above are potentially useful for distinguishing between BBOA and BSOA quantitatively and for advancing the characterization of their properties.

In this study, by analyzing the one-year filter samples collected at the Station for Measuring Ecosystem-Atmosphere Relations (SMEAR II) in the Hyytiälä forest, we differentiated between BBOA and BSOA in OAs and characterized their chemical structures through offline AMS analysis with increased chemical resolution by polarity-based fractionation. The Hyytiälä SMEAR II station is a rural site with low anthropogenic influence and strong biogenic emissions (Kulmala et al., 2001; Petäjä et al., 2021). This provides an ideal environment for investigating the chemical structural differences between BBOA and BSOA, as BSOA is difficult to identify and quantify when there are large contributions from BBOA or anthropogenic aerosols,

https://doi.org/10.5194/egusphere-2026-1023
Preprint. Discussion started: 16 March 2026

given that BSOA generally occur at much lower concentrations and are therefore easily masked by these stronger sources. The OA components in the samples were fractionated into HP-WSOM, HULIS, and WISOM fractions on the basis of their polarity, which is represented by their water solubility and affinity to an SPE column. Each fraction was analyzed by HR–AMS to determine the concentrations and chemical structural characteristics of OAs. PMF-based source apportionment was performed using the HR–AMS spectra, assisted by chemical structural information from methods developed in this study to distinguish between BBOA and BSOA factors. Then, the analyses were performed to investigate the seasonal variations in OA masses from different sources and how their solubility was influenced by their different chemical structures. The relative contributions of different OA fractions and the annual average OA concentration from this study were compared with those from other locations.

2 Methodology

2.1 Sample collection

Aerosol samples with diameters smaller than 0.95 μm ($PM_{0.95}$) were collected on quartz fiber filters using a high-volume air sampler (Model 120SL; Kimoto Electric Co., Ltd.) equipped with a cascade impactor (TE-234; Tisch Environmental, Inc.) at SMEAR II (Tarvainen et al., 2005), Hyytiälä Juupajoki, Finland (61°51′ N, 24°17′ E), from July 2021 to June 2022. Detailed sample information is provided in Table S1. Located in southern Finland, SMEAR II is surrounded by a boreal coniferous forest extending tens of kilometers to the north and northeast (Hellén et al., 2018). The area is sparsely populated and has limited local anthropogenic pollution sources, primarily household heating and cooking (Äijälä et al., 2017). A small residential and industrial area in Korkeakoski, located 6–7 km southeast of the sampling site, was reported to contain two sawmills and a pellet factory (Heikkinen et al., 2020; Liao et al., 2011; Ylivinkka et al., 2025). In summer, biogenic aerosols dominate in Hyytiälä, with additional contributions from transported pollution from continental Europe and western Russia, along with occasional influences from biomass burning emissions (Williams et al., 2011). A back trajectory analysis for the period of 1996–2008 indicated that clean air masses from the northwest favor new particle formation, whereas air masses from the southeast transport combustion-related accumulation-mode particles (Riuttanen et al., 2013). Anthropogenic pollution in the area mainly originates from industrial emissions in southern Finland and biomass burning in Russia and Eastern Europe (Yan et al., 2016; Heikkinen et al., 2021).

2.2 Extraction and fractionation

Twenty-four one-week samples, collected around the first and third weeks of each month, were subjected to the extraction of aerosol components. Two circular filter cuts (diameter: 34 mm) were taken from each filter sample for subsequent extraction. First, the punches were extracted three times using approximately 10 mL of water and 15 minutes of ultrasonication, followed by filtration through a 0.2-μm PTFE filter (Millex). Following WSOM extraction, the remaining filters were processed for WISOM extraction through sequential ultrasonication, first with 3 g of methanol, followed by three extractions using ~3.3 g

https://doi.org/10.5194/egusphere-2026-1023
Preprint. Discussion started: 16 March 2026

of a dichloromethane/methanol (2:1, v/v) mixture (Zhou et al., 2021).

A portion of the aqueous extract solution (4–6 g) was further processed by solid-phase extraction (SPE) to obtain HP-WSOM and HULIS (Varga et al., 2001) First, WSOM was acidified to pH 2 using 1 M HCl aqueous solution and passed through an Oasis HLB column (6 cc, 200 mg; Waters). The column was rinsed three times with 0.5 mL of 0.01 M HCl solution, and the resulting effluent was collected as HP-WSOM. Then, the HLB column was dried by N_2, after which the species adsorbed on the column were eluted with 6 mL of methanol to obtain HULIS. The details of the SPE extraction method can be found elsewhere (Zhou et al., 2021).

2.3 HR–AMS measurements and other analyses

The extract solutions of the OA fractions were nebulized using pure compressed air. The generated aerosols were then passed through diffusion driers with silica gel and activated carbon to remove solvent vapors. The carrier gas was subsequently replaced with high-purity Ar using a gas exchange device. Finally, the aerosol particles in the Ar flow were analyzed using a high-resolution time-of-flight aerosol mass spectrometer (Aerodyne Research, Inc.). The HR–AMS data were acquired in both V and W modes. The AMS data were analyzed using a ToF-AMS Analysis tool kit (Squirrel v1.65G) and a ToF-AMS HR Analysis tool kit (Pika v1.25G) template in Igor Pro (http://cires.colorado.edu/jimenez-group/ToFAMSResources/ToFSoftware/). The classification of fragment ions from organics to C_xH_y, $C_xH_yO_1$, $C_xH_yO_{>1}$, $C_xH_yN_z$, $C_xH_yON_z$, $C_xH_yO_{>1}N_z$, H_yO_q, and CS families and the elemental analysis to determine the O/C, H/C, and organic matter-to-organic carbon (OM/OC) ratios were performed using the Pika template. The extract solutions mixed with phthalic acid (PA) as an internal standard were also analyzed using the AMS in the same manner for the quantification of OAs (Mihara and Mochida, 2011).

For quantification, the least squares method was used to deconvolute the unit-mass OA spectrum of the mixture into the spectra of the extracts of OA and phthalic acid, providing the abundance of the extract relative to that of phthalic acid with a known amount (Mihara and Mochida, 2011). The five ions at m/z 28, 44, 50, 76, and 104 were excluded from the quantitative analysis of the WSOM and HP-WSOM samples to increase the fitting accuracy. The detailed rationale for the exclusion of these ions is provided in the Supplementary Information (Text S1). Because of the pH adjustment before SPE, the chemical states of HP-WSOM and HULIS may differ from their original forms in WSOM, potentially affecting their ionization efficiency in AMS. This may have led to fluctuations in the estimated extraction efficiency of SPE (Table S2), with some values slightly exceeding unity. Note that a calculated efficiency greater than unity has also been reported in previous studies (Afsana et al., 2022; Zhou et al., 2021).

A total organic carbon analyzer (Model TOC-VCSH, Shimadzu) was used to quantify the water-soluble organic carbon (WSOC) in the samples. The samples for the WSOC analysis were extracted separately from those used for the AMS analysis. The aerosol components on circular filter cuts (diameter: 28 mm) from each filter were extracted into 20 mL of water with two

https://doi.org/10.5194/egusphere-2026-1023
Preprint. Discussion started: 16 March 2026

15-minute ultrasonication cycles, followed by filtration through a disposable hydrophilic filter. Organic carbon (OC) and elemental carbon (EC) were analyzed for sample filter cuts (diameter: 8 mm) using a thermal/optical carbon analyzer (Model 2001A, Desert Research Institute) with the thermal/optical reflectance method following the IMPROVE temperature protocol. The abundance of OC was also derived from the HR–AMS analysis as the sum of carbon contents in WISOM, HULIS, and HP-WSOM, where their carbon contents were calculated by dividing their concentrations by their OM/OC ratios.

The quantified HR–AMS results were compared with the OC values from the thermal/optical analysis (Fig. S2 and Fig. S3a). The results indicate a strong correlation of the sum of water-insoluble organic carbon (WISOC), humic-like substances carbon (HULIS-C), and high-polarity water-soluble organic carbon (HP-WSOC) with the total OC (r = 0.987) (Fig. S3a) and the ratio of the former to the latter (mean ± SD: 1.33 ± 0.21). Additionally, the WSOC derived from AMS (HP-WSOM + HULIS) was in good agreement with the WSOC measured by the TOC analyzer, which is represented by a high correlation coefficient (r= 0.985; Fig. S3b) and the ratio of the former to the latter of 0.93 ±0.10 (mean ±SD). These results demonstrate the good accuracy and high extraction efficiency of our quantification method.

Meteorological parameters and atmospheric concentrations of two BVOCs, monoterpenes and MBO (2-methyl-3-buten-2-ol), from July 7, 2021, to June 22, 2022, which were measured at SMEARII and are available in the SmartSMEAR database (Junninen et al., 2009) , were averaged for each filter sampling period. The data sources included MBO (16.8 m), monoterpene (8.4 m), SO_2 (16.8 m), acetonitrile (125 m), solar radiation (35 m), and air temperature (16.8 m), all of which were obtained above ground level as quality-checked datasets (Aalto et al., 2025).

2.4 Back trajectory and PSCF analysis

Backward air mass trajectories were calculated using the HYSPLIT model with meteorological input from the NOAA Global Data Assimilation System (GDAS) (Draxler and Hess, 1997; Draxler, 1999; Stein et al., 2015; Draxler and Hess, 1998). All trajectories for the samples are provided in Figure S4. Each trajectory started at 500 m above sea level, with one 10-day (240 h) trajectory generated per sampling day at 12:00 UTC.

The potential source contribution function (PSCF) method based on backward trajectory analysis was employed to identify the potential source regions of particle pollution (Bressi et al., 2014; Jeong et al., 2011). Hourly trajectories over 168-hour periods were computed as inputs of the PSCF for the specific event periods. The hours with high concentrations of aerosols were defined using the 75th percentile of the particle volume concentration calculated using differential mobility particle sizer (DMPS) data for the 100–1000 nm size range, which were measured at SMEARII and are available in the SmartSMEAR database. The data processing procedures are described in Text S2.

https://doi.org/10.5194/egusphere-2026-1023
Preprint. Discussion started: 16 March 2026

2.5 PMF data processing

The W-mode HR–AMS data were imported into the Igor PMF template (PMF Evaluation Toolkit v3.08C) for the PMF analysis (Ulbrich et al., 2009a). The mass spectra of all four fractions, HP-WSOM, HULIS, WISOM, and WSOM, were processed together, and their corresponding error matrices were obtained from Pika. Five PMF solutions with fPeak and seed values of 0 and 1 were used for further analysis. Detailed results of the stability analysis for the PMF solutions, including the dependence of $Q/Q_{expected}$ on the number of factors, seed, and fPeak values, are provided in Figure S4. Among the PMF results, those for HP-WSOM, HULIS, and WISOM were selected for further data processing and analysis. Both four-factor and five-factor PMF solutions were tested, and each provided reasonable interpretations of the AMS spectra. To better capture the structural characteristics of the OA fractions, mainly a five-factor solution was used for the analysis in this study. The atmospheric concentrations of OA masses associated with the PMF factors were derived from the concentrations of OA fractions and the relative abundance of the PMF factors determined through the PMF analysis.

3 Results and discussion

3.1 Chemical structure of OA fractions

3.1.1 Composition and abundance of OA fractions

The average HR–AMS spectra of the three extracted fractions are shown in Fig. 1a. C_xH_y fragments representing hydrocarbon structures contributed as much as 63.7% of the WISOM. As the polarity increases in the order of WISOM, HULIS, and HP-WSOM, the contribution of C_xH_y decreases, whereas that of $C_xH_yO_1$ and $C_xH_yO_{>1}$ (representing mono- and multioxygenated organic fragments, respectively) increase. The distributions of the fragment ion groups of the three fractions were generally similar to those of urban aerosols from our previous study (Zhou et al., 2021): $C_xH_yO_1$ dominated in HP-WSOM; C_xH_y and $C_xH_yO_1$ were comparable in HULIS; and C_xH_y was most abundant in WISOM. The O/C and H/C ratios and the OM/OC mass ratio for WISOM, HULIS, and HP-WSOM are shown in Figure 1b. As the polarity increases in the order of WISOM, HULIS, and HP-WSOM, both the O/C and OM/OC ratios increase accordingly. HP-WSOM has the broadest range of O/C, H/C, and OM/OC values among the three fractions. The relative standard deviation of the O/C for HP-WSOM (24.4%) was also greater than that for HULIS (9.3%) and WISOM (16.1%), likely reflecting greater chemical diversity or variability of HP-WSOM across different samples.

https://doi.org/10.5194/egusphere-2026-1023
Preprint. Discussion started: 16 March 2026

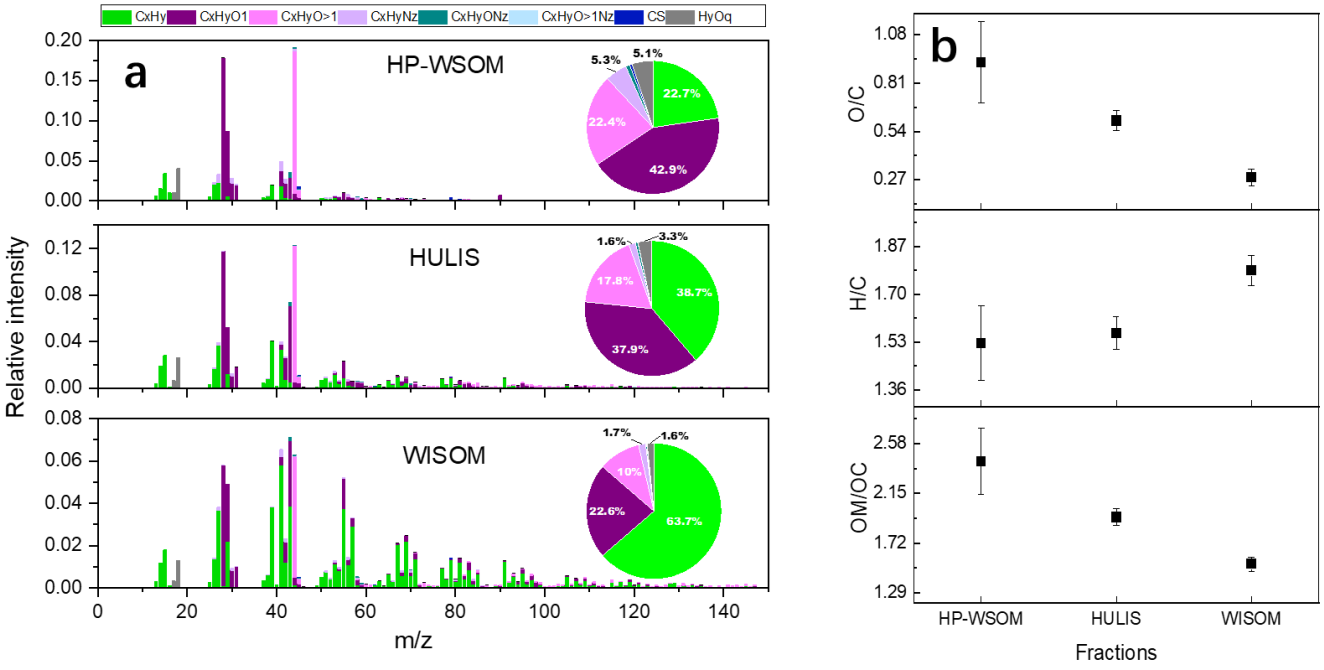

Figure 1(a) Averages of the normalized HR–AMS spectra for HP-WSOM, HULIS, and WISOM with pie charts showing the averages of the fractional contributions of fragment ion groups. Different fragment groups are represented by different colors in the stacked bars. (b) O/C and H/C ratios and OM/OC mass ratios of HP-WSOM, HULIS, and WISOM.

The seasonal variations in WISOM, HULIS, and HP-WSOM and the proportions of their averages are presented in Fig. 2a. The average and standard deviation of the total OA, calculated as the sum of the three fractions, was 1.24 ± 0.75 μg m^{-3}. With the exception of the two specific periods P1 (October 6 to 13) and P2 (March 9 to 16), with elevated concentrations of HULIS, OAs exhibited a clear seasonal pattern throughout the year. The mean OA concentrations in summer, autumn, winter, and spring were 2.06, 0.94, 0.62, and 1.34 μg/m^3, respectively. The higher OA concentration in summer than in winter is consistent with the seasonal variations in OAs observed in long-term ACSM data (2012–2018) at SMEAR II (Heikkinen et al., 2020). Among the OA fractions, HP-WSOM, HULIS, and WISOM also peaked in summer (0.25, 1.43, and 0.39 μg m^{-3}, respectively) and reached their minima in winter (0.13, 0.31, and 0.17 μg m^{-3}, respectively), which is consistent with the trend of total OAs.

https://doi.org/10.5194/egusphere-2026-1023
Preprint. Discussion started: 16 March 2026

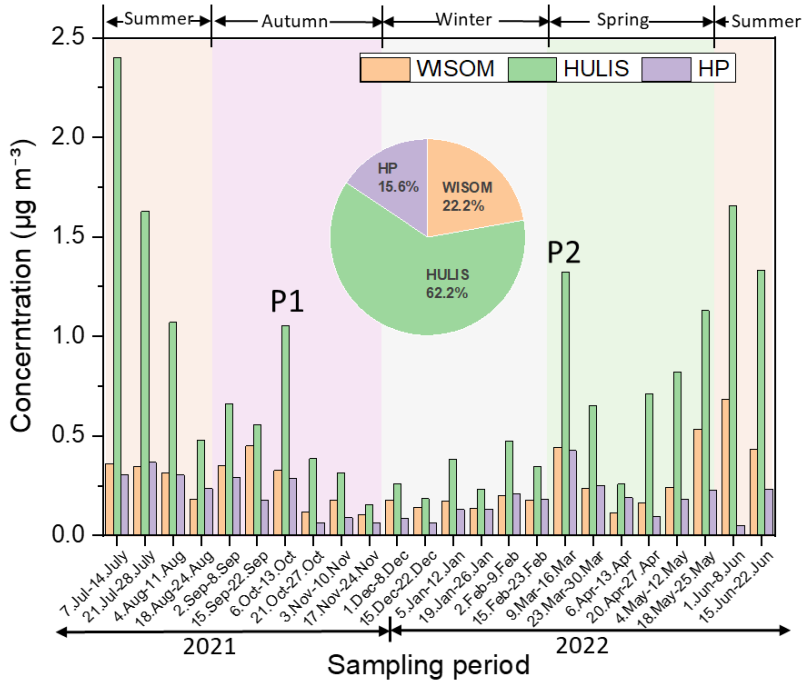

Figure 2 Seasonal variations in HP-WSOM, HULIS, and WISOM measured by HR–AMS, with the fractional contributions of their averages shown in the pie chart.

3.1.3 OA source regions during P1 and P2 events

To identify the potential source regions during the two events with elevated HULIS concentrations (P1 and P2), a PSCF analysis was performed using the 75th percentile of the particle volume concentration in the 100–1000 nm size range from the DMPS measurements. The calculated areas that were frequently traversed by the air masses that arrived at the study site during the high-concentration events are shown in Fig. 3.

In general, air masses passed over Scandinavia and other parts of Europe, and their passage over the North Atlantic Ocean and the Arctic Ocean was also evident. The potential source regions for the accumulation mode particles during P1 were located mainly southwest of the sampling site (Fig. 3a), with additional contributions from the southeast. The potential source regions for P2 were located mainly in the southeast. These spatial patterns are consistent with the findings of Riuttanen et al. (2013) who reported that clean air masses from the northwest were favorable for new particle formation, whereas air masses from the southeast were typically associated with combustion-related accumulation mode particles, on the basis of a long-term backward trajectory analysis from 1996 to 2008. The backward trajectory analysis (Fig. S6) reveals the possibility of long-range transport for P1, whereas P2 is characterized by circulation patterns over the estimated source regions depicted in Fig. 3b, which are

https://doi.org/10.5194/egusphere-2026-1023
Preprint. Discussion started: 16 March 2026

more conducive to the accumulation of pollutants. This may partly contribute to the higher OA concentration during P2 than during P1.

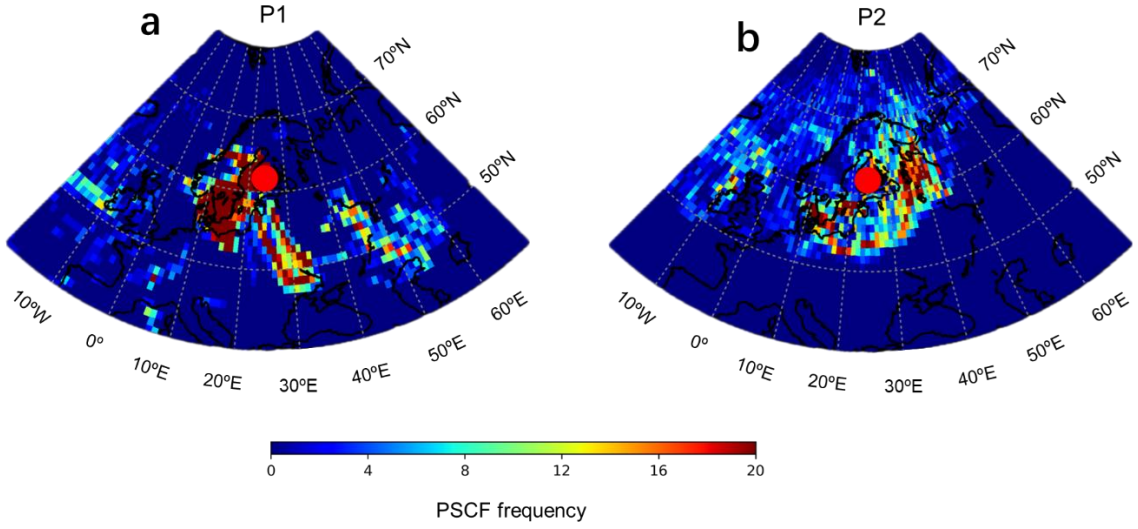

Figure 3 Potential source contribution function (PSCF) maps based on the 75th percentile of the DMPS-derived particle volume concentrations in the 100–1000 nm range. (a) P1 (October 6–13, 2021). (b) P2 (March 9–16, 2022).

3.2 PMF-derived OA types

3.2.1 Overview of source apportionment

Different apportionment techniques have been applied to deconvolve organic matter (OM) at the SMEAR II station into various sources, as summarized in Table 1 (Raatikainen et al., 2010; Yttri et al., 2011; Finessi et al., 2012; Crippa et al., 2014; Äijälä et al., 2017; Äijälä et al., 2019; Corrigan et al., 2013; Vogel et al., 2013; Jiang et al., 2019; Kortelainen et al., 2017; Zhang et al., 2024; Heikkinen et al., 2021). Commonly identified factors include semivolatile oxygenated organic aerosol (SVOOA), low-volatile oxygenated organic aerosol (LVOOA), biomass burning organic aerosol (BBOA), and hydrocarbon-like organic aerosol (HOA) factors. A previous study performed source apportionment of submicron aerosol particles in Hyytiälä, Finland, during July and August 2010 by using aerosol mass spectrometry and Fourier transform infrared spectroscopy (FT-IR). While the study identified four major components—biomass burning, biogenic sources, and two fossil fuel-related factors (Corrigan et al., 2013)—it highlighted a high similarity between BSOA and BBOA AMS spectra, indicating the need for methods to better differentiate them. In this study, by employing HR–AMS to analyze specific fragment ions at high resolution, we aim to extract compound type information that enables a more robust distinction between these two aerosol types. Notably, since an offline extraction method was applied, the same PMF factor across different fractions should represent chemical structures in

https://doi.org/10.5194/egusphere-2026-1023
Preprint. Discussion started: 16 March 2026

different sets of chemical species. As the focus of this work is on key chemical structures rather than on strict source attribution, we hereafter refer to them as BBOA-like and BSOA-like factors.

Table 1. Summary of source apportionment studies at the Hyytiälä forest station

Reference	Dataset	OA factors/types
(Raatikainen et al., 2010)	Q-AMS	OOA1, OOA2
(Yttri et al., 2011)	Thermal optical OC/EC, radiocarbon (^{14}C), HPLC–ESI–HRTOF-MS, GC	BSOA, BPAP, Fossil fuel, biomass burning
(Finessi et al., 2012)	Q-AMS, ToF-AMS, NMR	AMS: OOA1, OOA2 NMR: HULIS-containing, amines, terpene SOA-like
(Crippa et al., 2014)	AMS	HOA, BBOA, SVOOA, LVOOA
(Äijälä et al., 2017)	C-ToF-AMS	HOA, COA, SVOOA, LVOOA, sawmill SOA
(Äijälä et al., 2019)	ToF-AMS, C-ToF-AMS	Ammonium sulfate, ammonium nitrate, SVOOA, LVOOA, BBOA, nitrate-containing type, HOA
(Corrigan et al., 2013)	FT-IR, C-ToF-AMS	BSOA, BBOA, FFC1, FFC2
(Vogel et al., 2013)	AMS	OOA1, OOA2
(Jiang et al., 2019)	ACSM, AMS	HOA, BBOA, OOA
(Kortelainen et al., 2017)	HR–AMS	SV-OOA, LV-OOA and NO-factor
(Zhang et al., 2024)	LToF-AMS	Inorganic, OOA, HOA, BBOA, Kola pollution
(Heikkinen et al., 2021)	ACSM	SV-OOA, LV-OOA and POA
This study	HR–AMS	MO-OOA, BSOA-like, BBOA-like, CROA, HOA

3.2.2 PMF results

To investigate the potential sources of the three OA fractions (WISOM, HULIS, and HP-WSOM), we tested both four-factor and five-factor PMF solutions. The four-factor solution consisted of more-oxidized oxygenated organic aerosol (MO-OOA), BSOA-like factor, BSOA-like factor, and HOA, whereas the five-factor solution included these factors and an additional combustion-related organic aerosol (CROA) factor. The five-factor solution is used for further analysis in this study (Table 1). The time series and annual average contributions of the PMF factors are shown in Fig. 4. The factor with the lowest O/C ratio and the highest H/C ratio was associated with HOA, which were identified as the dominant component in WISOM, contributing 63% of WISOM on average. Moreover, MO-OOA, with the highest O/C ratio of 1.18, were the dominant component in HP-WSOM, accounting for 73.7% of HP-WSOM on average. These findings are consistent with our previous study, where HOA was also reported as a major contributor to WISOM (77%), and MO-OOA dominated the HP-WSOM fraction (96%) (Zhou et al., 2021). The source identification of the remaining three factors is discussed in detail in the following sections.

https://doi.org/10.5194/egusphere-2026-1023
Preprint. Discussion started: 16 March 2026

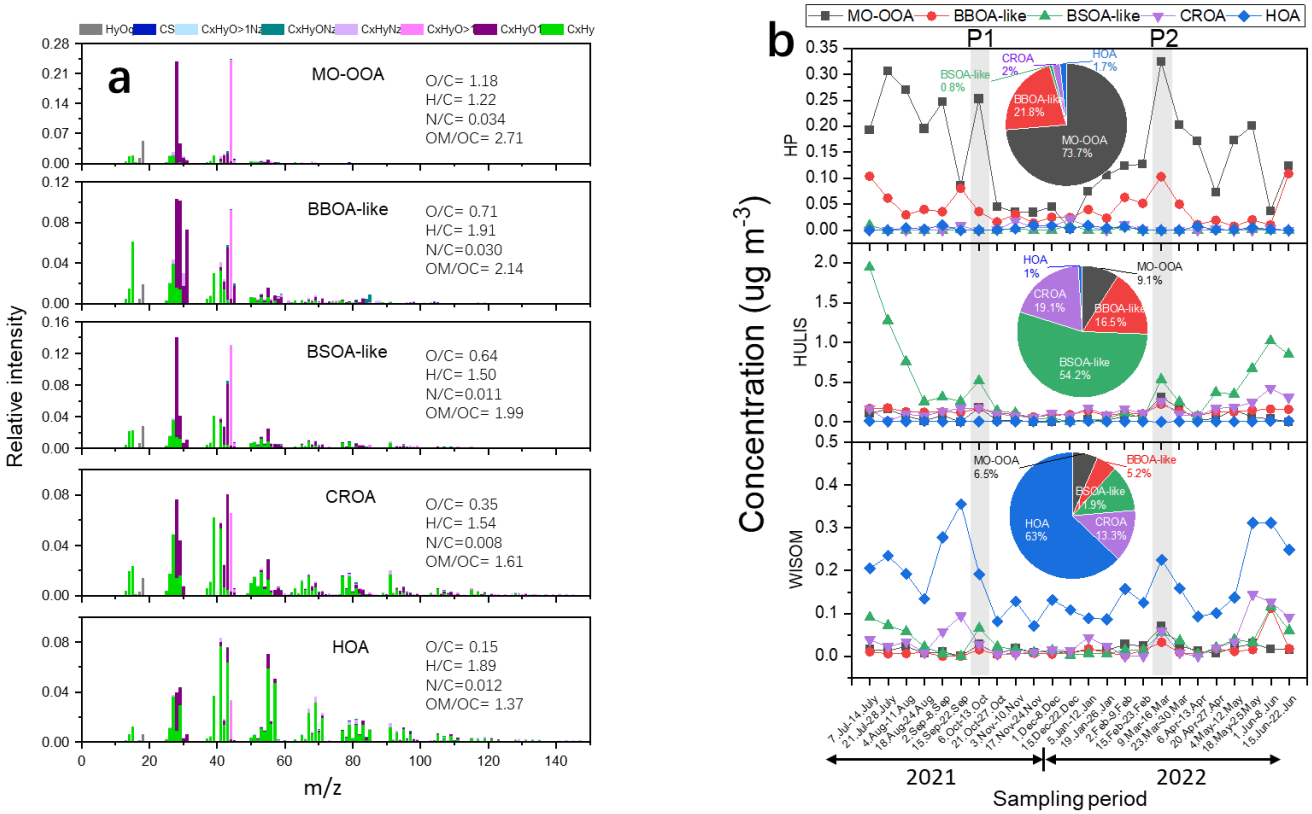

Figure 4. (a) HR–AMS spectra of the five PMF-derived factors and their elemental analysis data. (b) Time series of the concentrations of MO-OOA, BSOA-like, BSOA-like, CROA, and HOA in HP-WSOM, HULIS, and WISOM and the proportions of the mean concentrations.

3.2.3 BSOA-like tracers and related chemical structures

The identification of the BSOA-like factor is partly based on its characteristic seasonal pattern. During summer, BSOA-like factor accounted for up to 68.2% of HULIS, which is consistent with the enhanced BVOC emissions under higher temperatures and stronger solar radiation in summer than in the other seasons. The identification of the BSOA-like factor is further supported by the seasonal pattern closely resembling that of temperature and solar radiation (Fig. 5a). As shown in Figure 6, BSOA-like factor was strongly correlated with temperature (r = 0.83), solar radiation (r = 0.73), and MBO (a biogenic volatile organic compound primarily emitted by coniferous trees such as pines; r = 0.70), whereas the correlations with the other PMF factors were notably weaker. These correlations further support the biogenic secondary formation of the OA mass corresponding to the BSOA-like factor.

HOA was strongly correlated with MBO (r = 0.69) and showed the second strongest correlation with temperature (r = 0.55) and solar radiation (r = 0.55). Given that BVOCs are abundant in hydrocarbons, HOA is presumably influenced by both freshly

https://doi.org/10.5194/egusphere-2026-1023
Preprint. Discussion started: 16 March 2026

emitted biogenic aerosols and generally recognized fossil fuel combustion emissions. We observed that when OAs increased during P1 and P2, the concentrations of the BSOA-like factor also increased (Fig. 4b), suggesting a possible enhancing effect of anthropogenic pollution on BSOA.

To further investigate the chemical structural characteristics of the BSOA-like factor, we analyzed several fragment ions associated with the gaseous precursors (BVOCs). We selected $C_5H_7^+$ (m/z 67), $C_6H_9^+$ (m/z 81), and $C_7H_7^+$ (m/z 91) as representative medium-mass hydrocarbon-type markers since all have been reported as fragmentation ions characteristic of BSOA in several studies (Boyd et al., 2015; Bahreini et al., 2005; Kiendler-Scharr et al., 2009; Robinson et al., 2011). Although hydrocarbon-type fragment ions were detected at relatively high levels, they exhibited limited source specificity. Therefore, we also considered the higher mass but less abundant ions $C_7H_9O_3^+$ and $C_9H_{13}O_4^+$. The fragment ion $C_7H_9O_3^+$ (m/z 141) has been proposed as a signature for 3-methyl-1,2,3-butanetricarboxylic acid (MBTCA), a tracer compound indicative of terpene-derived SOAs (Kostenidou et al., 2018). $C_9H_{13}O_4^+$ (m/z 185) corresponds to the deprotonated form of $C_9H_{14}O_4$ terpenoic acids with a molecular weight of 186, such as cis-pinic acid (Yasmeen et al., 2011). $C_5H_6O^+$ (m/z 82) is a fragment ion widely recognized in field studies as a tracer for IEPOX-derived SOAs formed from isoprene oxidation under low-NO conditions, but it can also be substantially influenced by monoterpene-derived SOAs (Hu et al., 2015; Robinson et al., 2011).

These ions were strongly correlated with the BSOA-like factor, jointly supporting the identification of this factor, as presented in Fig. 5b. In this study, $C_5H_6O^+$ demonstrated high source specificity, showing a very strong correlation coefficient exclusively with the BSOA-like factor (r = 0.98). Although $C_5H_6O^+$ is generally regarded as a fragment ion that is indicative of isoprene oxidation, monoterpene-derived SOAs can also enhance its signal, as mentioned above (Hu et al., 2015). In addition, while monoterpenes dominate the mixing ratios during summer in Hyytiälä, the presence of isoprene is also evident (Hakola et al., 2012; Fischer et al., 2021). Therefore, both isoprene- and monoterpene-derived SOAs may be associated with the observed $C_5H_6O^+$ signal in this study. The medium-mass hydrocarbon-type fragment ions $C_5H_7^+$ (m/z 67), $C_6H_9^+$ (m/z 81), and $C_7H_7^+$ (m/z 91) also exhibited high correlations with the BSOA-like factor (r = 0.85, 0.76, and 0.88, respectively). However, their specificity as tracers of BBOA was limited. For example, HOA showed even stronger correlations with $C_5H_7^+$ and $C_6H_9^+$ than BSOA-like factor did, which is not unexpected because these two are hydrocarbon fragment ions. Therefore, these ions are unlikely to serve as BSOA tracers by themselves, but they could provide supportive evidence when used in combination with other marker ions. The abundance of higher-mass ions $C_7H_9O_3^+$ and $C_9H_{13}O_4^+$ was 1–2 orders of magnitude lower than that of the medium-mass ions mentioned, presumably because of extensive fragmentation under ~70 eV electron ionization(EI). Nevertheless, they exhibited notable source specificity and correlated strongly and exclusively with the BSOA-like factor (r: 0.95 and 0.93, respectively), with substantially weaker associations with other factors. $C_7H_9O_3^+$ and $C_9H_{13}O_4^+$ could therefore serve as characteristic signatures of BSOA-like factor in future EI-based mass spectrometric studies of OAs.

https://doi.org/10.5194/egusphere-2026-1023
Preprint. Discussion started: 16 March 2026

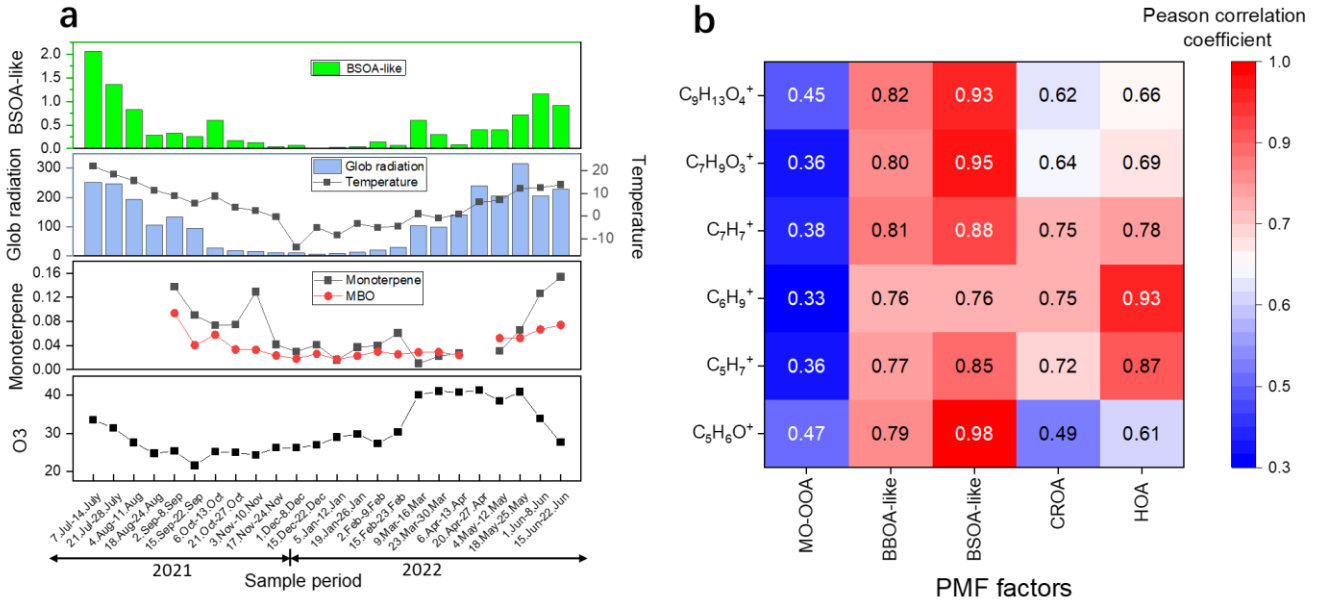

325 **Figure 5 (a) Time series of BSOA-like factor and $C_5H_8O_5^+$, along with those of global radiation, temperature, monoterpenes, MBO, and O3 (data from SmartSMEAR: https://smear.avaa.csc.fi/). (b) Correlation matrix illustrating the relationships between PMF-derived factors and characteristic fragment ions.**

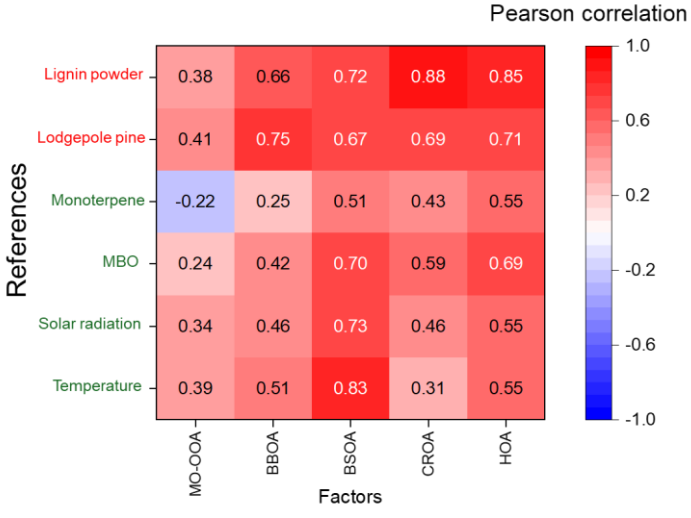

Figure 6. Pearson correlation coefficients between PMF-resolved OA factors and six selected references. The references include two 330 **meteorological parameters (temperature and solar radiation, data from SmartSMEAR), two BVOCs (monoterpene and MBO, also from SmartSMEAR), and two biomass burning HR–AMS spectra (from the AMS Spectral Database, URL: http://cires.colorado.edu/jimenez-group/AMSsd/) (Ulbrich et al., 2009b).**

https://doi.org/10.5194/egusphere-2026-1023
Preprint. Discussion started: 16 March 2026

3.2.4 BBOA-like tracers and related chemical structures

To confirm the identification of the BBOA-like factor, we compared the UMR spectra of five PMF factors with the AMS spectrum of aerosols from chamber-burned lodgepole pine (needles and sticks) from the AMS spectral database (Ulbrich et al., 2009b) (Fig. S6a). The BBOA-like factor exhibited the highest correlation coefficient (r = 0.75) among the five PMF factors (Fig. 6), supporting its association with BBOA.

The time series of non-sea-salt (nss)-SO_4^{2-} and nss-K^+ from ion chromatography are shown in Figure 7. The nss-K^+ concentration is widely used as an indicator of the influence of biomass burning, although it could also be affected by other sources, such as agricultural activities and soil resuspension (Andreae, 1983; Zhang et al., 2010). Despite a weak correlation with the BBOA-like factor (r = 0.30), nss-K^+ exhibited a pronounced increase during P1 and a smaller increase during P2, whereas other cations did not show similar patterns, suggesting episodic biomass-burning influences. The sources of nss-SO_4^{2-} are complex and generally represent secondary inorganic aerosols generated from anthropogenic sulfur dioxide, marine biogenic precursors, volcanic emissions and so forth (Seinfeld and Pandis, 2016). Although its correlation with the BBOA-like factor was modest (r = 0.45), nss-SO_4^{2-} increased during both P1 and P2 and exhibited a temporal pattern similar to that of the BBOA-like time series, whereas other anions did not show comparable variations, suggesting that biomass burning may have contributed to the sulfate concentration in addition to fossil fuel combustion.

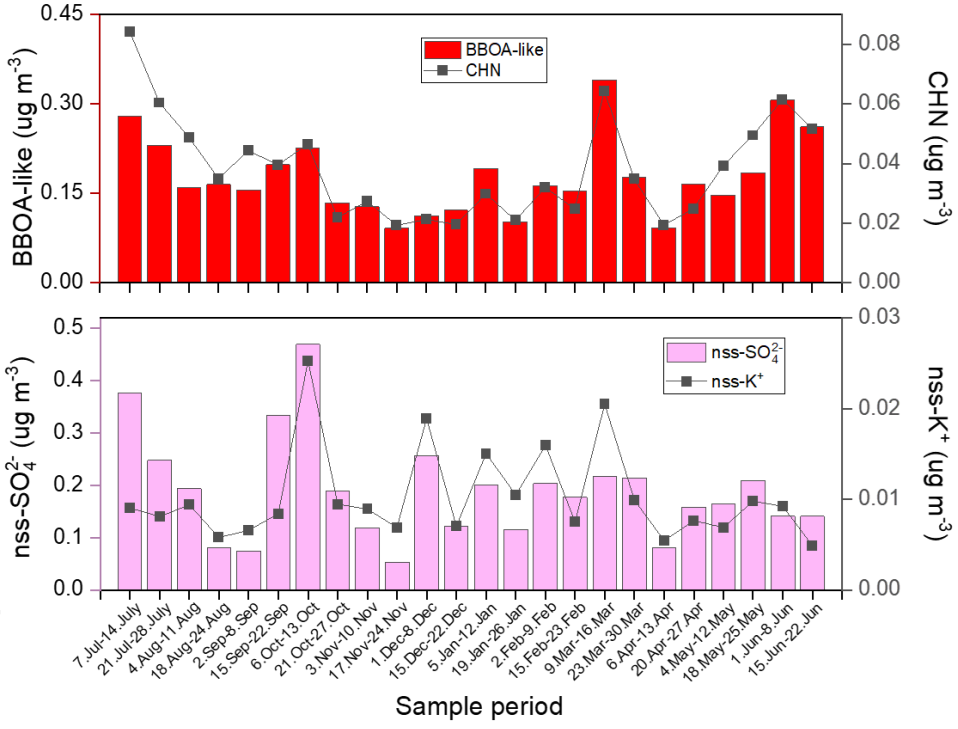

Figure 7. Time series of BBOA-like factor, CHN family ions, nss-SO_4^{2-} and nss-K^+.

https://doi.org/10.5194/egusphere-2026-1023
Preprint. Discussion started: 16 March 2026

As explained in the introduction section, BBOA generally contain NOC fragment ions from both CHN and CHON family compounds, whereas BSOA predominantly consist of CHON family compounds formed through the oxidation and nitration of BVOCs (Laskin et al., 2014; Laskin et al., 2009). On the basis of this distinction, we consider that CHN family ions can serve as tracers for differentiating BBOA from BSOA. As shown in Fig. 7, the concentration of the BBOA-like factor exhibits a variation pattern closely aligned with that of the CHN family, with a high correlation coefficient (r = 0.85).

To further investigate the characteristics of the CHN family compounds, we listed all CHN family ions quantified and calculated their corresponding annual average concentrations, as shown in Fig. 8a. The distribution of the CHN family ions among the three OA fractions revealed the high water solubility of the compounds from which they originated. An average of 76.3% of the total CHN family ions were from water-soluble compounds, and smaller ions tended to originate more from water-soluble compounds. Among the CHN family ions, CHN^+, CH_4N^+, and $C_2H_3N^+$ were the most abundant. Previous chamber and field studies have reported that CH_4N^+ can serve as a tracer ion for amines (Ge et al., 2024) and that $C_nH_{2n-1}N^+$ and $C_nH_{2n-2}N^+$ are likely associated with nitriles (Ge et al., 2024; Mclafferty and Turecek, 1993). The presence of amines and nitriles supports the proposed formation pathway of CHN family compounds in BBOA, as outlined in the introduction: high-temperature biomass combustion facilitates the release of ammonia and amines, followed by reactions with carboxylic acids to form alkyl amides and subsequent dehydration to produce alkyl nitriles.

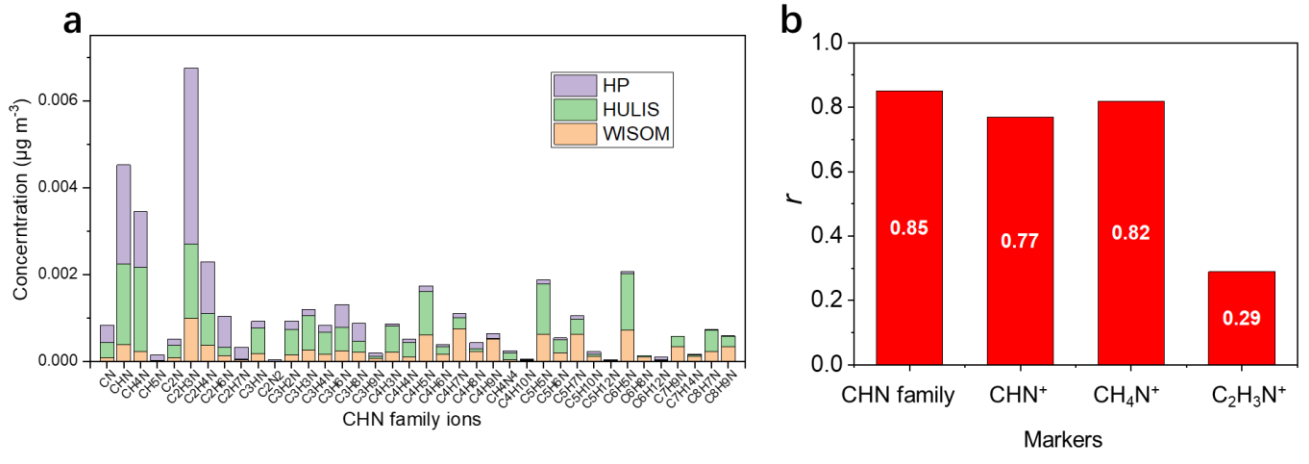

Figure 8 (a) Annual average concentrations of the OA mass detected as different CHN family ions in HP-WSOM, HULIS, and WISOM. (b) Correlation coefficients of the time series of BBOA-like factor with the series of total CHN family ions and individual ions (CHN^+, CH_4N^+, and $C_2H_3N^+$).

https://doi.org/10.5194/egusphere-2026-1023
Preprint. Discussion started: 16 March 2026

This study also considers the performance of the tracer ion from levoglucosan, $C_2H_4O_2^+$ (m/z 60). Previous studies conducted at Hyytiälä suggested that m/z 60 is difficult to observe at this site because of degradation during long-range transport (Corrigan et al., 2013; Zhang et al., 2024). The signal of $C_2H_4O_2^+$ or m/z 60, both in their studies and in this study, was rarely observed in the spectra of the PMF factors. However, when the HR mode data were examined, clear variations in the $C_2H_4O_2^+$ ion concentration became evident. Thus, the time series of the $C_2H_4O_2^+$ ion intensity from the HR–AMS data was compared with the time series of the BBOA-like factor, as shown in Fig. 9. The results demonstrate that the temporal pattern of the BBOA-like factor closely resembles that of $C_2H_4O_2^+$ with a higher correlation coefficient (r = 0.93) than other factors (MO-OOA: 0.59; BSOA-like: 0.84; CROA: 0.66; HOA: 0.68). This strong association provides additional evidence for the robustness of the BBOA-like factor identification and for the validity of $C_2H_4O_2^+$ as a tracer of biomass burning emissions.

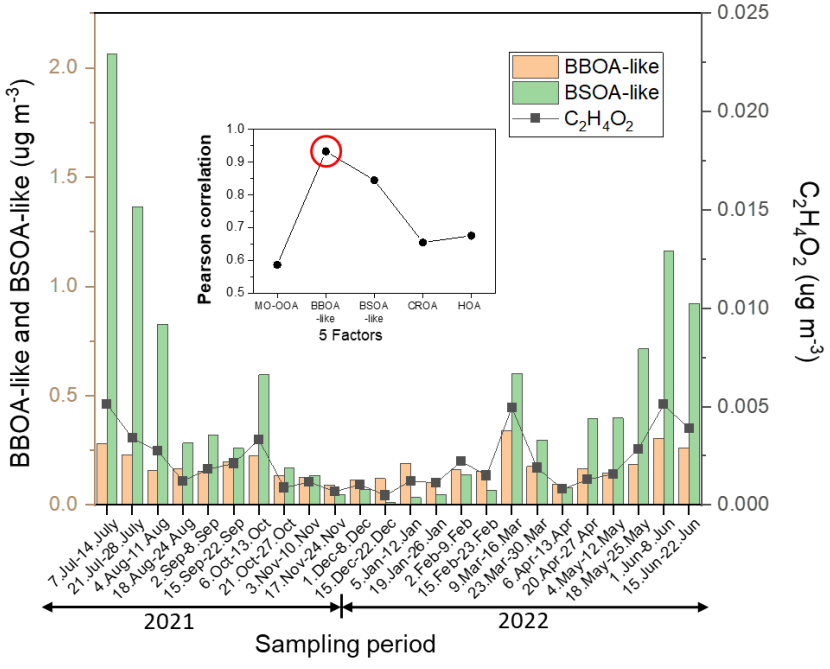

Figure 9. Temporal variations in the BBOA-like factor, BSOA-like factor, and $C_2H_4O_2^+$ during different sampling periods, with the inset showing the Pearson correlation coefficients between $C_2H_4O_2^+$ and the five PMF factors.

3.2.5 Comparison of BBOA-like, CROA and BSOA-like structures

Although both the CROA and BBOA-like factors are considered to be related to combustion sources, the structural differences between the CROA and BBOA-like factors are clear. The mass spectra of these two factors in Fig. 10 show that CROA are characterized by aromatic fragment ions, such as $C_6H_5^+$ (m/z 77), $C_6H_7^+$ (m/z 79), and $C_7H_7^+$ (m/z 91). One possible explanation is that the CROA factor is related to aged OAs originating from fossil fuel emissions. Whereas a PMF factor associated with

https://doi.org/10.5194/egusphere-2026-1023
Preprint. Discussion started: 16 March 2026

fresh OAs from fossil fuel combustion, as a type of POA, typically results in a low O/C ratio, for example, 0.14 in central eastern China (Hu et al., 2017) and 0.17 in Beijing (Zhou et al., 2021), the CROA factor in this study shows a higher O/C ratio of 0.35. Moreover, OAs from fossil fuel are expected to be distributed primarily in WISOM (Zhou et al., 2021), whereas in our case, 79.5% (annual average) of the CROA mass was found in the HULIS fraction, suggesting a higher water solubility, which is consistent with the higher degree of oxidation.

Another explanation is that the CROA factor originated from the combustion of aged biomass materials. This finding is supported by a recent study (Ma et al., 2024), which proposed that the composition of OAs originating from biomass burning emissions can be classified into two types: OAs from the combustion of fresh biomass and OAs from the combustion of aged biomass. Fresh biomass, such as vegetation burned in forest fires, is typically rich in nutrients, including lipids and proteins. As discussed in Section 3.2.4, our BBOA-like factor is characterized by CHN family ions, including CHN^+ (*m/z* 27), CH_4N^+ (*m/z* 30), and $C_2H_3N^+$ (*m/z* 41), which are indicative of the combustion of protein-rich fresh biomass. In contrast, aged biomass, including postharvest straw, fallen leaves, and deadwood, is generally nutrient poor, with abundant lignin (Ma et al., 2024). The pyrolysis or combustion of lignin releases large amounts of aromatic compounds (Simoneit, 2002), as evidenced by aromatic peaks in the reference spectrum of lignin powder retrieved from the AMS spectral database (Ulbrich et al., 2009b) (Fig. S6b). Among the five PMF factors, the CROA factor exhibits the highest spectral similarity with lignin combustion (r = 0.88), exceeding those of the MO-OOA (r = 0.38), BBOA-like (r = 0.66), BSOA-like (r = 0.72), and HOA (r = 0.85) factors, supporting its association with lignin-rich sources. Furthermore, as shown in Fig. 4a, the N/C ratio of the BBOA-like factor (0.03) was substantially higher than that of the CROA factor (0.008). These findings suggest that BBOA-like compounds are closely associated with the combustion of fresh biomass, whereas the aromatic character of CROA is linked to fossil fuel-derived OAs and/or the burning of aged biomass.

The N/C ratio of BSOA-like factor (0.011) lies between the ratios of BBOA-like and CROA factors, which may be attributed to the formation of oxygen- and nitrogen-containing organic compounds (NOCs) via the oxidation and nitration of biogenic VOCs (BVOCs). In addition, the mass spectral profile of BSOA-like factor also contains signals of aromatic-like fragment ions such as $C_6H_5^+$ (m/z 77), $C_6H_7^+$ (m/z 79), and $C_7H_7^+$ (m/z 91), although their intensities are much weaker than those of CROA. Similar features have been observed in the HR–AMS spectra from chamber experiments of SOAs generated from α-pinene ozonolysis and oxidation under high-NO_x conditions (Chhabra et al., 2011; Chhabra et al., 2010), indicating that the presence of aromatic-like signals (potentially derived from nonaromatic precursors) in BSOA-like factor is not unexpected. In the higher m/z range (100–150), the differences between BSOA-like and CROA factors become more evident: CROA is dominated by C_xH_y family ions, contributing 41.3% of the total signal compared with 24.1% in BSOA-like factor, whereas BSOA-like factor is enriched in $C_xH_yO_{>1}$ ions, reaching 42.6% compared with 24.9% in CROA.

https://doi.org/10.5194/egusphere-2026-1023
Preprint. Discussion started: 16 March 2026

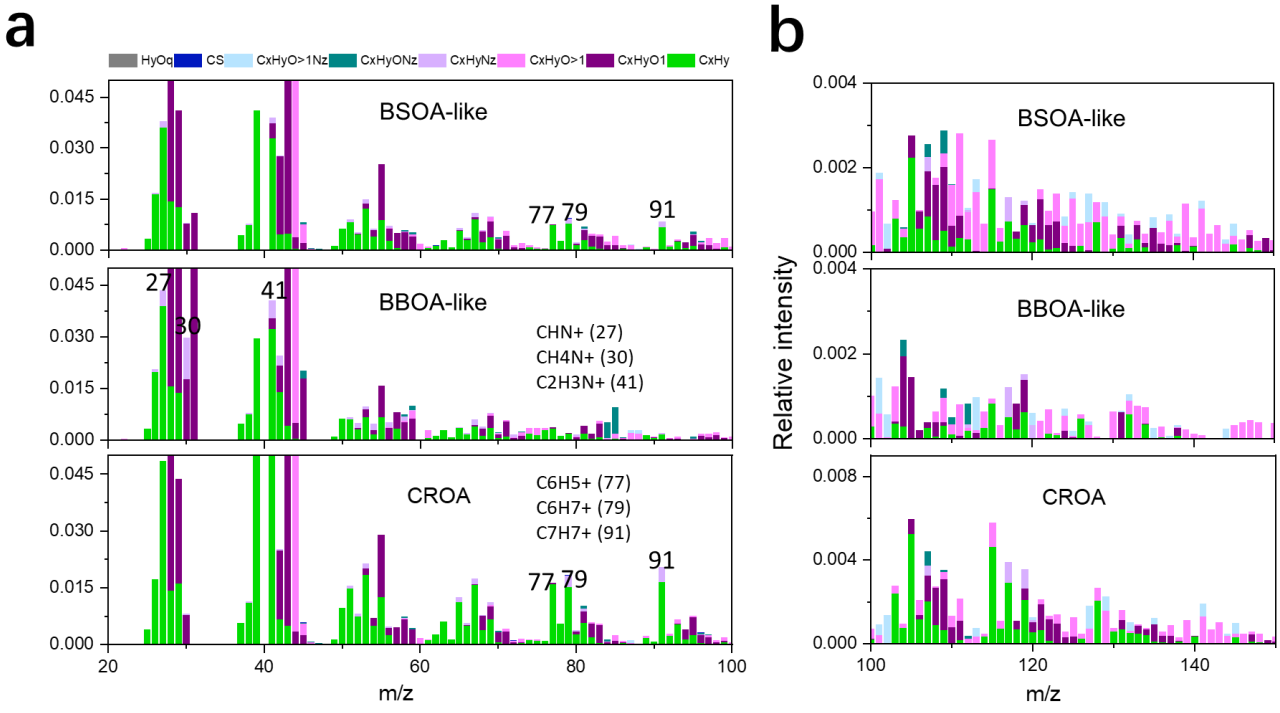

Figure 10. (a) Enlarged mass spectra of the BSOA-like, BBOA-like, and CROA factors with annotated characteristic fragment ions in the m/z range 20–100 (some prominent peaks are outside the vertical axis range). (b) Enlarged mass spectra of the BSOA-like, BBOA-like, and CROA factors in the m/z range of 100–150.

3.3 Application of PMF for fractionation-based offline AMS analysis

3.3.1 PMF factors

The seasonal variations in the relative contributions of the five PMF factors throughout the year are shown in Figure 11. Among them, the BSOA-like factor was the only factor that exhibited a clear summertime maximum and wintertime minimum, with its mean seasonal contribution reaching 49% in summer, indicating that BSOA-like factor were the dominant contributors to OAs during this period. In Hyytiälä, the average temperature for the respective filter sampling periods exceeded 20 °C only during the first sampling period (July 7–14), when the average temperature reached 21.8 °C (Fig. 5a). During this period, BSOA-like factor accounted for 66.7% of the total OAs, which was the highest among the studied periods.

In contrast to BSOA-like factor, BBOA-like factor and CROA factor exhibited opposite seasonal variation patterns, with peaks of seasonal average contributions of 25% and 24% in winter, respectively, and lower contributions of 12% and 11% during summer, respectively. In addition, the mass contributions of BBOA-like factor and CROA factor were correlated throughout the year (r = 0.63). On the basis of previous studies, the combustion-related aerosols observed at Hyytiälä are predominantly

https://doi.org/10.5194/egusphere-2026-1023
Preprint. Discussion started: 16 March 2026

435 transferred by air masses from the southeast (Riuttanen et al., 2013).

HOA exhibited the greatest relative contributions in autumn and winter, both of which reached 22% on average, likely reflecting increased fossil fuel consumption due to residential heating during cold months. In contrast, MO-OOA did not show a pronounced seasonal pattern; MO-OOA contribution peaked in spring and reached 27% on average, which may be associated with enhanced photochemical activity due to long daylight hours and elevated levels of atmospheric oxidants such as ozone
440 (Fig. 5a).

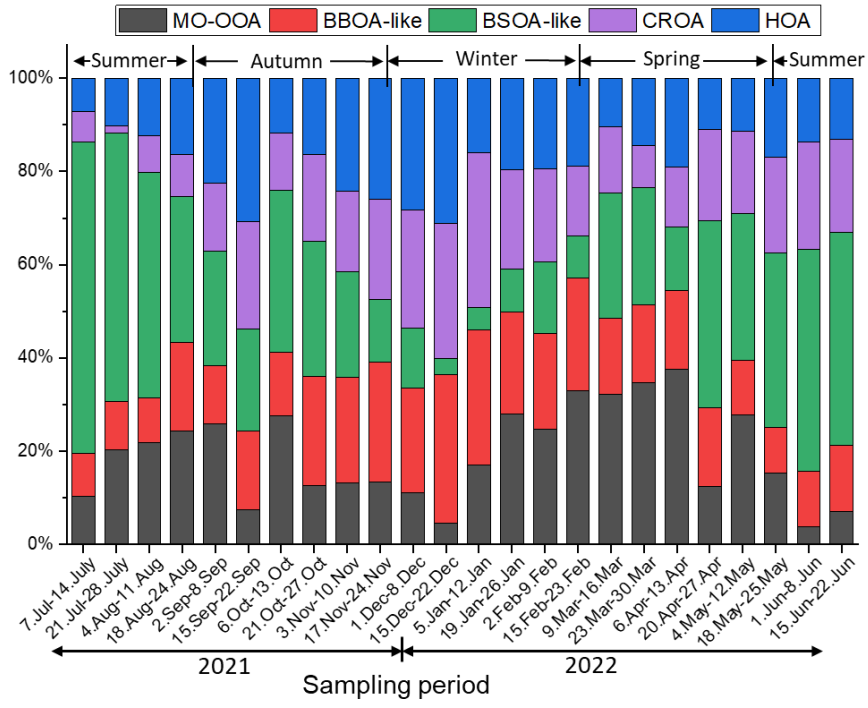

Figure 11. Relative contributions of PMF factors to total OAs.

3.3.2 Solubility analysis with PMF factors

The time series of the proportions of the water-insoluble fractions of the five PMF factors, which are based on the
445 concentrations of the PMF factors in the three OA fractions, are shown in Figure 12. The majority of HOA was distributed in the WISOM fraction, with an annual average of 92.4%, and the proportion remained quite stable throughout the sampling period. The water-insoluble fraction of CROA fluctuated more throughout the year, with an annual average of 17.8%, but was generally higher than that of BBOA-like factor (mean: 7.0%). The difference between CROA and BBOA-like factors is likely associated with the distinct structural characteristics of the two factors: BBOA-like factor is enriched in CHN family
450 compounds, which are generally hydrophilic, whereas CROA shows stronger signals of aromatic species, which are relatively hydrophobic. The annual average water-insoluble fraction of MO-OOA was 11.1%, indicating the water-soluble characteristics

https://doi.org/10.5194/egusphere-2026-1023
Preprint. Discussion started: 16 March 2026

of the compounds associated with this factor. Notably, the data point from 15–22 December was abnormally high, which may have been affected by experimental uncertainty because of the very low concentrations of all three fractions (Fig. 4b).

The annual average water-insoluble fraction of compounds associated with the BSOA-like factor was 10.8%, which also indicated water-soluble characteristics. Owing to the very low fraction of the BSOA-like factor in winter, large uncertainties may exist during this period. If the winter values are excluded, the WISOM fraction was 8.4% on average. Previous chamber and field studies have demonstrated that BSOA is generally mostly water soluble. For instance, the soluble fraction of isoprene-derived SOAs has been reported to exceed 80% (Xu et al., 2017), whereas that of limonene-derived SOAs generated in chamber experiments may exceed 95% (Bateman et al., 2010). The results of the present study are in reasonable agreement with those of previous studies.

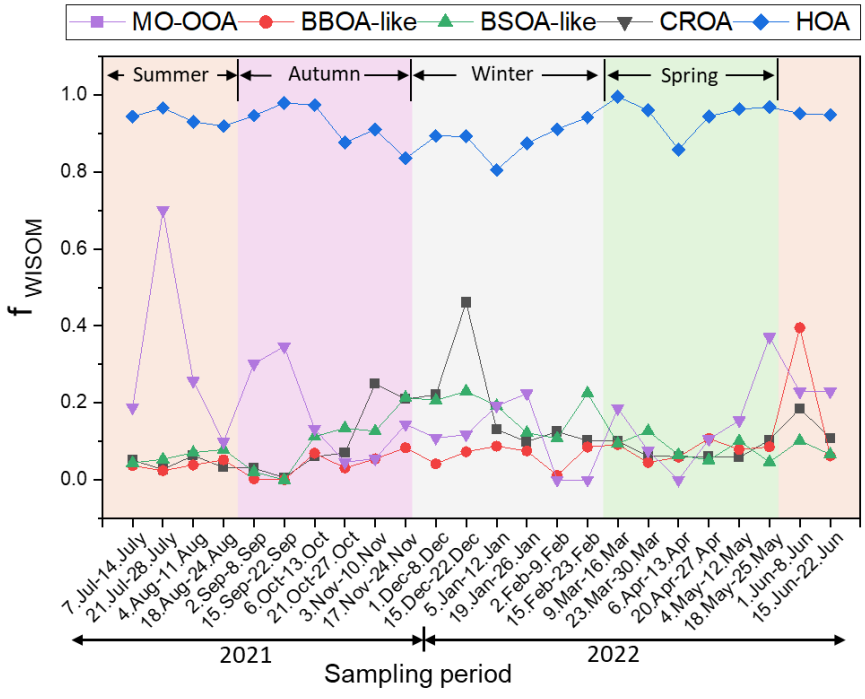

Figure 12. Seasonal variations in the water-insoluble fraction of the five PMF factors.

3.3.3 Polarity distribution analysis with PMF factors

The seasonal variations in the proportions of HP-WSOM, HULIS, and WISOM are presented in Fig. 13a. The seasonal variation patterns reveal that HULIS dominated in summer and made a lower contribution in winter. According to a previous study, fossil fuel emissions are the dominant contributor to WISOM across all seasons in urban environments (Zhou et al., 2021). In Hyytiälä, WISOM showed the greatest seasonal contribution in winter, reaching 30.4%, followed by autumn (28.2%), spring (22.1%), and summer (19.8%). This seasonality likely reflects increased inputs of fossil fuel-derived aerosols in winter,

https://doi.org/10.5194/egusphere-2026-1023
Preprint. Discussion started: 16 March 2026

whereas the reduced WISOM fraction in summer may be attributed to the absence of fossil fuel usage for residential heating, along with the enhanced formation of BBOA, which primarily contributed to the HULIS fraction. The OC/EC ratios from the thermal/optical analysis exhibited a pronounced seasonal pattern, with the highest mean value of 6.72 in summer (Fig. S2b), indicating a significant contribution of secondary OAs. In contrast, the lowest mean OC/EC value of 1.61 was observed in the winter. This finding indicates the enhanced influence of fossil fuel-derived aerosols, including EC, during winter and explains the increased WISOM fraction.

The pie charts in Figure 13b show the annual mean proportions of HP-WSOM, HULIS, and WISOM at Hyytiälä (Finland) and two other sites: Tomakomai (Japan) and Beijing (China). The three sampling sites are considered to represent a gradient of anthropogenic influence: Hyytiälä in Finland is a boreal forest background site with minimal local emissions; the Tomakomai experimental forest (TOEF) in Hokkaido, Japan, is a cool-temperate forest site subject to regional and moderate anthropogenic influence; and Beijing, China, is a megacity strongly affected by fossil fuel combustion and other human activities. The OA concentrations at the three sites tended to increase with increasing degree of anthropogenic influence, with mean annual values of 1.2, 1.6, and 34.6 μg m^{-3} at Hyytiälä, Tomakomai, and Beijing, respectively. At the clean forest site of Hyytiälä, HULIS constituted the dominant fraction, accounting for 64%, followed by WISOM (23%) and HP-WSOM (13%). A similar distribution but with a lower proportion of HULIS was reported for the forest site of Tomakomai, where HULIS accounted for 51%, WISOM accounted for 29%, and HP-WSOM accounted for 20% (Afsana et al., 2022). The proportions of urban aerosols in Beijing markedly differed, with WISOM accounting for 45%, followed by HP-WSOM (32%) and HULIS (23%) (Zhou et al., 2021). Source apportionment based on the PMF analysis in the present study can help explain this difference. In forest regions, particularly in summer, the BSOA-like factor contributes substantially to HULIS, whereas such a contribution is not expected in urban areas. In the case of WISOM, which is strongly associated with fossil fuel OAs, traffic emissions in densely populated urban areas should contribute heavily. As a result, forested regions, especially in summer, were dominated by HULIS, whereas WISOM accounted for the greatest fraction in urban areas.

https://doi.org/10.5194/egusphere-2026-1023
Preprint. Discussion started: 16 March 2026

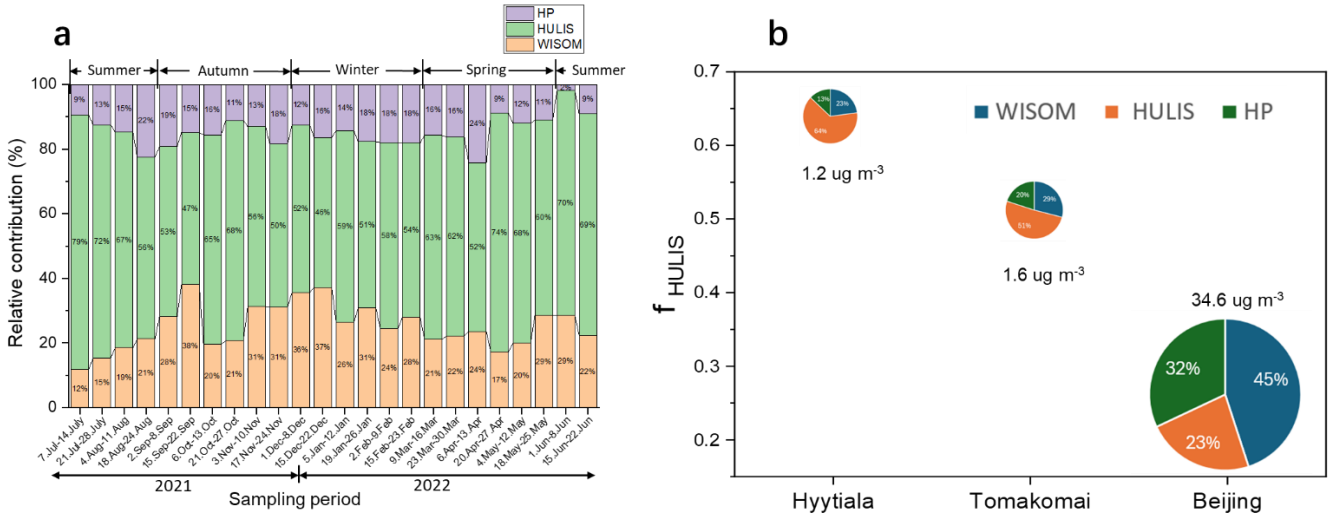

Figure 13 (a) Relative contributions of HP-WSOM, HULIS, and WISOM to total OAs. (b) Annual mean values of the proportions of HP-WSOM, HULIS, and WISOM with annual average OA concentrations at three sites in Hyytiälä, Tomakomai, and Beijing.

4. Summary and conclusions

In this study, offline chemical structure analysis and PMF-based source apportionment of OAs in a boreal coniferous forest in Finland were performed. The samples were extracted into three fractions of varying polarities: HP-WSOM, HULIS, and WISOM. This study is based on sampling in four different seasons and shows clear seasonal patterns of the concentrations of OA fractions and total OAs, with higher and lower levels in summer and winter, respectively. HR–AMS data combined with PMF identified five factors and quantified their distributions among the three OA fractions: the MO-OOA, BBOA-like, BSOA-like, CROA, and HOA factors. The BSOA-like factor exhibited a pronounced seasonal pattern, peaking in summer and showing strong correlations with temperature and solar radiation. The BSOA-like factor was the dominant contributor to the HULIS fraction, accounting for 54.2%.

In this work, a series of methods based on previous studies were developed to characterize the chemical structure of different factors, especially for BBOA and BSOA. We identified several nonhydrocarbon ions, including $C_5H_6O^+$, $C_7H_9O_3^+$ and $C_9H_{13}O_4^+$, as potential BSOA-like compound markers. Despite their low signal intensities, these ions showed high specificity for the BSOA-like factor and could serve as markers of BSOA in future atmospheric research by EI mass spectrometry. The time series of the levoglucosan signal ($C_2H_4O_2^+$) showed the strongest correlation with the BBOA-like factor, supporting the identification of the source type of BBOA. This study also explored CHN family ions as potential BBOA-like factor markers for the first time, revealing a strong correlation on a mass fraction basis. By analyzing the three most abundant ions in the CHN family, CHN^+, CH_4N^+, and $C_2H_3N^+$, we interpreted their occurrence as indicating the emissions from protein-rich biomass combustion and the subsequent formation of CHN family species. In addition, we identified CROA factor, characterized by

https://doi.org/10.5194/egusphere-2026-1023
Preprint. Discussion started: 16 March 2026

aromatic compounds, and considered their sources to be fossil fuel OAs and/or the combustion of aged biomass.

Finally, polarity-based analysis combined with PMF was performed. The BSOA-like PMF factor dominated in summer, whereas the BBOA-like, CROA, and HOA factors increased during colder seasons. HOA was almost water-insoluble, CROA was more hydrophobic than BBOA-like factor due to its aromatic composition, whereas BSOA-like and MO-OOA factors were mainly water soluble. A comparison across different sites revealed that compared with urban aerosols, forest aerosols had lower OA concentrations but higher proportions of HULIS. This difference is explained by the greater abundance of BSOA in forest environments, which were present mainly in the HULIS fraction.

Overall, the results of this study demonstrate that HR–AMS fragment ions help to distinguish sources such as BBOA and BSOA, providing potential markers for future EI-based mass spectrometric research. The results also highlight the importance of long-term observations and systematic analysis of the polarity-resolved source apportionment in advancing our understanding of the chemical complexity of OAs. In this study, the different distributions of the BBOA-like and BSOA-like factors among the three OA fractions demonstrate the distinction between these two structures. The PMF factors identified in this study are better interpreted as dynamic mixtures of submolecular structures rather than fixed sets of organic compounds, which may also be the case for the PMF factors reported in previous conventional online studies. Looking ahead, extending the source apportionment results based on chemical structural differences to investigations of the properties related to the roles of OA in climate and air quality would be valuable.

Data availability

The data for this study are presented in this manuscript and the supporting information material, and additional data will be available in the Zenodo data repository (https://zenodo.org/).

Author contributions

QS and MM jointly conceptualized the study and designed the experiments. LA, TP, SO, and MK contributed to the use of the SMEAR II station for aerosol sampling. QS and CS performed the experiments with contributions from RZ and MM. QS analyzed the data with contributions from MM and prepared the manuscript with contributions from MM, RZ, TP, and IY.

Competing interests

Tuukka Petäjä is an editor of *Atmospheric Chemistry and Physics*. The authors declare that they have no other conflicts of interest.

Acknowledgments

This work was financially supported by JSPS KAKENHI (JP23H00515 and JP19KK0265) and JST SPRING (JPMJSP2125). The first author also gratefully acknowledges support from the “Interdisciplinary Frontier Next-Generation Researcher

https://doi.org/10.5194/egusphere-2026-1023
Preprint. Discussion started: 16 March 2026

Program" of the Tokai Higher Education and Research System. Funding through ACTRIS-IMP Transnational Access is gratefully acknowledged. The technical staff of SMEAR II are gratefully acknowledged for their support during measurements and sampling. The operation of SMEAR II is financially supported by the University of Helsinki and Research Council of Finland through INAR RI (345510, 358647, 367739) and ACCC flagship (337549, 357902, 359340). The authors gratefully acknowledge NOAA's Air Resources Laboratory (ARL) for providing the HYSPLIT transport and dispersion model and the READY website used in this study.

References

Aalto, J., Aalto, P., Keronen, P., Kolari, P., Rantala, P., Taipale, R., Kajos, M., Patokoski, J., Rinne, J., Ruuskanen, T., Leskinen, M., Laakso, H., Levula, J., Pohja, T., Siivola, E., Kulmala, M., and Ylivinkka, I.: SMEAR II Hyytiälä forest meteorology, greenhouse gases, air quality and soil, FAIRDATA Etsin [dataset], https://doi.org/10.23729/fd-933fd9fd-d31b-3e26-a01b-acef7901b843, 2025.

Afsana, S., Zhou, R., Miyazaki, Y., Tachibana, E., Deshmukh, D. K., Kawamura, K., and Mochida, M.: Abundance, chemical structure, and light absorption properties of humic-like substances (HULIS) and other organic fractions of forest aerosols in Hokkaido, Scientific Reports, 12, 14379, https://doi.org/10.1038/s41598-022-18201-z, 2022.

Äijälä, M., Daellenbach, K. R., Canonaco, F., Heikkinen, L., Junninen, H., Petäjä, T., Kulmala, M., Prévôt, A. S. H., and Ehn, M.: Constructing a data-driven receptor model for organic and inorganic aerosol – a synthesis analysis of eight mass spectrometric data sets from a boreal forest site, Atmos. Chem. Phys., 19, 3645-3672, https://doi.org/10.5194/acp-19-3645-2019, 2019.

Äijälä, M., Heikkinen, L., Fröhlich, R., Canonaco, F., Prévôt, A. S. H., Junninen, H., Petäjä, T., Kulmala, M., Worsnop, D., and Ehn, M.: Resolving anthropogenic aerosol pollution types – deconvolution and exploratory classification of pollution events, Atmos. Chem. Phys., 17, 3165-3197, https://doi.org/10.5194/acp-17-3165-2017, 2017.

Andreae, M. O.: Soot Carbon and Excess Fine Potassium: Long-Range Transport of Combustion-Derived Aerosols, Science, 220, 1148-1151, https://doi.org/10.1126/science.220.4602.1148, 1983.

Bahreini, R., Keywood, M. D., Ng, N. L., Varutbangkul, V., Gao, S., Flagan, R. C., Seinfeld, J. H., Worsnop, D. R., and Jimenez, J. L.: Measurements of Secondary Organic Aerosol from Oxidation of Cycloalkenes, Terpenes, and m-Xylene Using an Aerodyne Aerosol Mass Spectrometer, Environmental Science & Technology, 39, 5674-5688, https://doi.org/10.1021/es048061a, 2005.

Bateman, A. P., Nizkorodov, S. A., Laskin, J., and Laskin, A.: High-Resolution Electrospray Ionization Mass Spectrometry Analysis of Water-Soluble Organic Aerosols Collected with a Particle into Liquid Sampler, Analytical Chemistry, 82, 8010-8016, https://doi.org/10.1021/ac1014386, 2010.

Boyd, C. M., Sanchez, J., Xu, L., Eugene, A. J., Nah, T., Tuet, W. Y., Guzman, M. I., and Ng, N. L.: Secondary organic aerosol formation from the β-pinene+NO₃ system: effect of humidity and peroxy radical fate, Atmos. Chem. Phys., 15, 7497-7522, https://doi.org/10.5194/acp-15-7497-2015, 2015.

Bressi, M., Sciare, J., Ghersi, V., Mihalopoulos, N., Petit, J. E., Nicolas, J. B., Moukhtar, S., Rosso, A., Féron, A., Bonnaire, N., Poulakis, E., and Theodosi, C.: Sources and geographical origins of fine aerosols in Paris (France), Atmos. Chem. Phys., 14, 8813-8839, https://doi.org/10.5194/acp-14-8813-2014, 2014.

Chen, Q., Ikemori, F., Higo, H., Asakawa, D., and Mochida, M.: Chemical Structural Characteristics of HULIS and Other Fractionated Organic Matter in Urban Aerosols: Results from Mass Spectral and FT-IR Analysis, Environ Sci Technol, 50, 1721-1730, https://doi.org/10.1021/acs.est.5b05277, 2016.

Chen, Q., Ikemori, F., Nakamura, Y., Vodicka, P., Kawamura, K., and Mochida, M.: Structural and Light-Absorption Characteristics of Complex Water-Insoluble Organic Mixtures in Urban Submicrometer Aerosols, Environmental Science & Technology, 51, 8293-8303, https://doi.org/10.1021/acs.est.7b01630, 2017.

https://doi.org/10.5194/egusphere-2026-1023
Preprint. Discussion started: 16 March 2026

Chen, W., Yang, H., Chen, Y., Li, K., Xia, M., and Chen, H.: Influence of Biochar Addition on Nitrogen Transformation during Copyrolysis of Algae and Lignocellulosic Biomass, Environmental Science & Technology, 52, 9514-9521, https://doi.org/10.1021/acs.est.8b02485, 2018.

Cheng, Y., Ma, Y., and Hu, D.: Tracer-based source apportioning of atmospheric organic carbon and the influence of anthropogenic emissions on secondary organic aerosol formation in Hong Kong, Atmos. Chem. Phys., 21, 10589-10608, https://doi.org/10.5194/acp-21-10589-2021, 2021.

Cheng, Y., He, K.-b., Du, Z.-y., Engling, G., Liu, J.-m., Ma, Y.-l., Zheng, M., and Weber, R. J.: The characteristics of brown carbon aerosol during winter in Beijing, Atmospheric Environment, 127, 355-364, https://doi.org/10.1016/j.atmosenv.2015.12.035, 2016.

Chhabra, P. S., Flagan, R. C., and Seinfeld, J. H.: Elemental analysis of chamber organic aerosol using an aerodyne high-resolution aerosol mass spectrometer, Atmos. Chem. Phys., 10, 4111-4131, https://doi.org/10.5194/acp-10-4111-2010, 2010.

Chhabra, P. S., Ng, N. L., Canagaratna, M. R., Corrigan, A. L., Russell, L. M., Worsnop, D. R., Flagan, R. C., and Seinfeld, J. H.: Elemental composition and oxidation of chamber organic aerosol, Atmos. Chem. Phys., 11, 8827-8845, https://doi.org/10.5194/acp-11-8827-2011, 2011.

Corrigan, A. L., Russell, L. M., Takahama, S., Äijälä, M., Ehn, M., Junninen, H., Rinne, J., Petäjä, T., Kulmala, M., Vogel, A. L., Hoffmann, T., Ebben, C. J., Geiger, F. M., Chhabra, P., Seinfeld, J. H., Worsnop, D. R., Song, W., Auld, J., and Williams, J.: Biogenic and biomass burning organic aerosol in a boreal forest at Hyytiälä, Finland, during HUMPPA-COPEC 2010, Atmos. Chem. Phys., 13, 12233-12256, https://doi.org/10.5194/acp-13-12233-2013, 2013.

Crippa, M., Canonaco, F., Lanz, V. A., Äijälä, M., Allan, J. D., Carbone, S., Capes, G., Ceburnis, D., Dall'Osto, M., Day, D. A., DeCarlo, P. F., Ehn, M., Eriksson, A., Freney, E., Hildebrandt Ruiz, L., Hillamo, R., Jimenez, J. L., Junninen, H., Kiendler-Scharr, A., Kortelainen, A. M., Kulmala, M., Laaksonen, A., Mensah, A. A., Mohr, C., Nemitz, E., O'Dowd, C., Ovadnevaite, J., Pandis, S. N., Petäjä, T., Poulain, L., Saarikoski, S., Sellegri, K., Swietlicki, E., Tiitta, P., Worsnop, D. R., Baltensperger, U., and Prévôt, A. S. H.: Organic aerosol components derived from 25 AMS data sets across Europe using a consistent ME-2 based source apportionment approach, Atmos. Chem. Phys., 14, 6159-6176, https://doi.org/10.5194/acp-14-6159-2014, 2014.

Deng, Y., Yai, H., Fujinari, H., Kawana, K., Nakayama, T., and Mochida, M.: Diurnal variation and size dependence of the hygroscopicity of organic aerosol at a forest site in Wakayama, Japan: their relationship to CCN concentrations, Atmospheric Chemistry and Physics, 19, 5889-5903, 10.5194/acp-19-5889-2019, 2019.

Draxler, R. R.: HYSPLIT4 user's guide, NOAA Air Resources Laboratory, Silver Spring, MD, NOAA Tech. Memo. ERL ARL-230, 1999.

Draxler, R. R. and Hess, G. D.: Description of the HYSPLIT_4 modeling system, NOAA Air Resources Laboratory, Silver Spring, MD, NOAA Tech. Memo. ERL ARL-224, 1997.

Draxler, R. R. and Hess, G. D.: An overview of the HYSPLIT_4 modeling system of trajectories, dispersion, and deposition, Australian Meteorological Magazine, 47, 295-308, 1998.

Duarte, R. M. B. O. and Duarte, A. C.: A critical review of advanced analytical techniques for water-soluble organic matter from atmospheric aerosols, TrAC Trends in Analytical Chemistry, 30, 1659-1671, https://doi.org/10.1016/j.trac.2011.04.020, 2011.

Dusek, U., Hitzenberger, R., Kasper-Giebl, A., Kistler, M., Meijer, H. A. J., Szidat, S., Wacker, L., Holzinger, R., and Röckmann, T.: Sources and formation mechanisms of carbonaceous aerosol at a regional background site in the Netherlands: insights from a year-long radiocarbon study, Atmos. Chem. Phys., 17, 3233-3251, 10.5194/acp-17-3233-2017, 2017.

Finessi, E., Decesari, S., Paglione, M., Giulianelli, L., Carbone, C., Gilardoni, S., Fuzzi, S., Saarikoski, S., Raatikainen, T., Hillamo, R., Allan, J., Mentel, T. F., Tiitta, P., Laaksonen, A., Petäjä, T., Kulmala, M., Worsnop, D. R., and Facchini, M. C.: Determination of the biogenic secondary organic aerosol fraction in the boreal forest by NMR spectroscopy, Atmos. Chem. Phys., 12, 941-959, 10.5194/acp-12-941-2012, 2012.

Fischer, L., Breitenlechner, M., Canaval, E., Scholz, W., Striednig, M., Graus, M., Karl, T. G., Petäjä, T., Kulmala, M., and Hansel, A.: First eddy covariance flux measurements of semi-volatile organic compounds with the PTR3-TOF-MS, Atmos. Meas. Tech., 14, 8019-8039, https://doi.org10.5194/amt-14-8019-2021, 2021.

Ge, X., Sun, Y., Trousdell, J., Chen, M., and Zhang, Q.: Enhancing characterization of organic nitrogen components in aerosols and droplets using high-resolution aerosol mass spectrometry, Atmos. Meas. Tech., 17, 423-439, https://doi.org/10.5194/amt-17-423-2024, 2024.

https://doi.org/10.5194/egusphere-2026-1023
Preprint. Discussion started: 16 March 2026

Gelencsér, A., May, B., Simpson, D., Sánchez-Ochoa, A., Kasper-Giebl, A., Puxbaum, H., Caseiro, A., Pio, C., and Legrand, M.: Source apportionment of PM2.5 organic aerosol over Europe: Primary/secondary, natural/anthropogenic, and fossil/biogenic origin, Journal of Geophysical Research: Atmospheres, 112, https://doi.org/10.1029/2006JD008094, 2007.

Gilardoni, S., Vignati, E., Cavalli, F., Putaud, J. P., Larsen, B. R., Karl, M., Stenström, K., Genberg, J., Henne, S., and Dentener, F.: Better constraints on sources of carbonaceous aerosols using a combined ¹⁴C – macro tracer analysis in a European rural background site, Atmos. Chem. Phys., 11, 5685-5700, https://doi.org/10.5194/acp-11-5685-2011, 2011.

Guenther, A. B., Jiang, X., Heald, C. L., Sakulyanontvittaya, T., Duhl, T., Emmons, L. K., and Wang, X.: The Model of Emissions of Gases and Aerosols from Nature version 2.1 (MEGAN2.1): an extended and updated framework for modeling biogenic emissions, Geosci. Model Dev., 5, 1471-1492, https://doi.org/10.5194/gmd-5-1471-2012, 2012.

Gysel, M., Weingartner, E., Nyeki, S., Paulsen, D., Baltensperger, U., Galambos, I., and Kiss, G.: Hygroscopic properties of water-soluble matter and humic-like organics in atmospheric fine aerosol, Atmos. Chem. Phys., 4, 35-50, https://doi.org/10.5194/acp-4-35-2004, 2004.

Hakola, H., Hellén, H., Hemmilä, M., Rinne, J., and Kulmala, M.: In situ measurements of volatile organic compounds in a boreal forest, Atmos. Chem. Phys., 12, 11665-11678, https://doi.org/10.5194/acp-12-11665-2012, 2012.

Haque, M. M., Verma, S. K., Deshmukh, D. K., Kunwar, B., and Kawamura, K.: Seasonal characteristics of biogenic secondary organic aerosol tracers in a deciduous broadleaf forest in northern Japan, Chemosphere, 311, 136785, https://doi.org/10.1016/j.chemosphere.2022.136785, 2023.

Heikkinen, L., Äijälä, M., Daellenbach, K. R., Chen, G., Garmash, O., Aliaga, D., Graeffe, F., Räty, M., Luoma, K., Aalto, P., Kulmala, M., Petäjä, T., Worsnop, D., and Ehn, M.: Eight years of sub-micrometre organic aerosol composition data from the boreal forest characterized using a machine-learning approach, Atmospheric Chemistry and Physics, 21, 10081-10109, https://doi.org/10.5194/acp-21-10081-2021, 2021.

Heikkinen, L., Äijälä, M., Riva, M., Luoma, K., Dällenbach, K., Aalto, J., Aalto, P., Aliaga, D., Aurela, M., Keskinen, H., Makkonen, U., Rantala, P., Kulmala, M., Petäjä, T., Worsnop, D., and Ehn, M.: Long-term sub-micrometer aerosol chemical composition in the boreal forest: inter- and intra-annual variability, Atmos. Chem. Phys., 20, 3151-3180, https://doi.org/10.5194/acp-20-3151-2020, 2020.

Hellén, H., Praplan, A. P., Tykkä, T., Ylivinkka, I., Vakkari, V., Bäck, J., Petäjä, T., Kulmala, M., and Hakola, H.: Long-term measurements of volatile organic compounds highlight the importance of sesquiterpenes for the atmospheric chemistry of a boreal forest, Atmospheric Chemistry and Physics, 18, 13839-13863, https://doi.org/10.5194/acp-18-13839-2018, 2018.

Hennigan, C. J., Sullivan, A. P., Collett Jr., J. L., and Robinson, A. L.: Levoglucosan stability in biomass burning particles exposed to hydroxyl radicals, Geophysical Research Letters, 37, https://doi.org/10.1029/2010GL043088, 2010.

Hu, W., Hu, M., Hu, W. W., Zheng, J., Chen, C., Wu, Y., and Guo, S.: Seasonal variations in high time-resolved chemical compositions, sources, and evolution of atmospheric submicron aerosols in the megacity Beijing, Atmos. Chem. Phys., 17, 9979-10000, https://doi.org/10.5194/acp-17-9979-2017, 2017.

Hu, W. W., Campuzano-Jost, P., Palm, B. B., Day, D. A., Ortega, A. M., Hayes, P. L., Krechmer, J. E., Chen, Q., Kuwata, M., Liu, Y. J., de Sá, S. S., McKinney, K., Martin, S. T., Hu, M., Budisulistiorini, S. H., Riva, M., Surratt, J. D., St. Clair, J. M., Isaacman-Van Wertz, G., Yee, L. D., Goldstein, A. H., Carbone, S., Brito, J., Artaxo, P., de Gouw, J. A., Koss, A., Wisthaler, A., Mikoviny, T., Karl, T., Kaser, L., Jud, W., Hansel, A., Docherty, K. S., Alexander, M. L., Robinson, N. H., Coe, H., Allan, J. D., Canagaratna, M. R., Paulot, F., and Jimenez, J. L.: Characterization of a real-time tracer for isoprene epoxydiols-derived secondary organic aerosol (IEPOX-SOA) from aerosol mass spectrometer measurements, Atmos. Chem. Phys., 15, 11807-11833, https://doi.org/10.5194/acp-15-11807-2015, 2015.

Jeong, U., Kim, J., Lee, H., Jung, J., Kim, Y. J., Song, C. H., and Koo, J.-H.: Estimation of the contributions of long range transported aerosol in East Asia to carbonaceous aerosol and PM concentrations in Seoul, Korea using highly time resolved measurements: a PSCF model approach, Journal of Environmental Monitoring, 13, 1905-1918, 10.1039/C0EM00659A, 2011.

Jiang, J., Aksoyoglu, S., El-Haddad, I., Ciarelli, G., Denier van der Gon, H. A. C., Canonaco, F., Gilardoni, S., Paglione, M., Minguillón, M. C., Favez, O., Zhang, Y., Marchand, N., Hao, L., Virtanen, A., Florou, K., O'Dowd, C., Ovadnevaite, J., Baltensperger, U., and Prévôt, A. S. H.: Sources of organic aerosols in Europe: a modeling study using CAMx with modified volatility basis set scheme, Atmos. Chem. Phys., 19, 15247-15270, https://doi.org/10.5194/acp-19-15247-2019, 2019.

Jolleys, M. D., Coe, H., McFiggans, G., Taylor, J. W., O'Shea, S. J., Le Breton, M., Bauguitte, S. J. B., Moller, S., Di Carlo, P., Aruffo, E., Palmer, P. I., Lee, J. D., Percival, C. J., and Gallagher, M. W.: Properties and evolution of biomass burning organic aerosol from Canadian boreal forest fires, Atmos. Chem. Phys., 15, 3077-3095, 10.5194/acp-15-3077-2015, 2015.

https://doi.org/10.5194/egusphere-2026-1023
Preprint. Discussion started: 16 March 2026

Junninen, H., Lauri, A., Keronen, P., Aalto, P., Hiltunen, V., Hari, P., and Kulmala, M.: Smart-SMEAR: on-line data exploration and visualization tool for SMEAR stations, Boreal Environment Research, 14, 447, 2009.

Kiendler-Scharr, A., Zhang, Q., Hohaus, T., Kleist, E., Mensah, A., Mentel, T. F., Spindler, C., Uerlings, R., Tillmann, R., and Wildt, J.: Aerosol Mass Spectrometric Features of Biogenic SOA: Observations from a Plant Chamber and in Rural Atmospheric Environments, Environmental Science & Technology, 43, 8166-8172, https://doi.org/10.1021/es901420b, 2009.

Kortelainen, A., Hao, L., Tiitta, P., Jaatinen, A., Miettinen, P., Kulmala, M., Smith, J. N., Laaksonen, A., Worsnop, D. R., and Virtanen, A.: Sources of particulate organic nitrates in the boreal forest in Finland, 2017.

Kostenidou, E., Karnezi, E., Kolodziejczyk, A., Szmigielski, R., and Pandis, S. N.: Physical and Chemical Properties of 3-Methyl-1,2,3-butanetricarboxylic Acid (MBTCA) Aerosol, Environmental Science & Technology, 52, 1150-1155, https://doi.org/10.1021/acs.est.7b04348, 2018.

KULMALA, M., HÄMERI, K., Aalto, P., Mäkelä, J., PIRJOLA, L., Nilsson, E. D., Buzorius, G., Rannik, Ü., Maso, M. D., and Seidl, W.: Overview of the international project on biogenic aerosol formation in the boreal forest (BIOFOR), Tellus B, 53, 324-343, https://doi.org/10.1034/j.1600-0889.2001.530402.x, 2001.

Laskin, A., Smith, J. S., and Laskin, J.: Molecular Characterization of Nitrogen-Containing Organic Compounds in Biomass Burning Aerosols Using High-Resolution Mass Spectrometry, Environmental Science & Technology, 43, 3764-3771, https://doi.org/10.1021/es803456n, 2009.

Laskin, J., Laskin, A., Nizkorodov, S. A., Roach, P., Eckert, P., Gilles, M. K., Wang, B., Lee, H. J., and Hu, Q.: Molecular Selectivity of Brown Carbon Chromophores, Environmental Science & Technology, 48, 12047-12055, https://doi.org/10.1021/es503432r, 2014.

Li, Y., Fu, T.-M., Yu, J. Z., Zhang, A., Yu, X., Ye, J., Zhu, L., Shen, H., Wang, C., Yang, X., Tao, S., Chen, Q., Li, Y., Li, L., Che, H., and Heald, C. L.: Nitrogen dominates global atmospheric organic aerosol absorption, Science, 387, 989-995, https://doi.org/10.1126/science.adr4473, 2025.

Liao, L., Dal Maso, M., Taipale, R., Rinne, J., Ehn, M., Junninen, H., Äijälä, M., Nieminen, T., Alekseychik, P., and Hulkkonen, M.: Monoterpene pollution episodes in a forest environment: indication of anthropogenic origin and association with aerosol particles, Boreal environment research, 16, 288, 2011.

Lin, P., Huang, X.-F., He, L.-Y., and Zhen Yu, J.: Abundance and size distribution of HULIS in ambient aerosols at a rural site in South China, Journal of Aerosol Science, 41, 74-87, https://doi.org/10.1016/j.jaerosci.2009.09.001, 2010.

Liu, C., Chung, C. E., Zhang, F., and Yin, Y.: The colors of biomass burning aerosols in the atmosphere, Scientific Reports, 6, 28267, https://doi.org/10.1038/srep28267, 2016.

Ma, Y. J., Xu, Y., Yang, T., Xiao, H. W., and Xiao, H. Y.: Measurement report: Characteristics of nitrogen-containing organics in PM2.5 in Ürümqi, northwestern China – differential impacts of combustion of fresh and aged biomass materials, Atmos. Chem. Phys., 24, 4331-4346, https://doi.org/10.5194/acp-24-4331-2024, 2024.

McLafferty, F. W. and Turecek, F.: Interpretation of mass spectra, University science books1993.

Mihara, T. and Mochida, M.: Characterization of Solvent-Extractable Organics in Urban Aerosols Based on Mass Spectrum Analysis and Hygroscopic Growth Measurement, Environmental Science & Technology, 45, 9168-9174, https://doi.org/10.1021/es201271w, 2011.

Müller, A., Aoki, K., Tachibana, E., Hiura, T., and Miyazaki, Y.: Impact of biogenic emissions of organic matter from a cool-temperate forest on aerosol optical properties, Atmospheric environment, 229, 117413, https://doi.org/10.1016/j.atmosenv.2020.117413, 2020.

Petäjä, T., Tabakova, K., Manninen, A., Ezhova, E., O'Connor, E., Moisseev, D., Sinclair, V. A., Backman, J., Levula, J., Luoma, K., Virkkula, A., Paramonov, M., Räty, M., Äijälä, M., Heikkinen, L., Ehn, M., Sipilä, M., Yli-Juuti, T., Virtanen, A., Ritsche, M., Hickmon, N., Pulik, G., Rosenfeld, D., Worsnop, D. R., Bäck, J., Kulmala, M., and Kerminen, V. M.: Influence of biogenic emissions from boreal forests on aerosol–cloud interactions, Nature Geoscience, 15, 42-47, 10.1038/s41561-021-00876-0, 2021.

Qin, M., Hu, Y., Wang, X., Vasilakos, P., Boyd, C. M., Xu, L., Song, Y., Ng, N. L., Nenes, A., and Russell, A. G.: Modeling biogenic secondary organic aerosol (BSOA) formation from monoterpene reactions with NO3: A case study of the SOAS campaign using CMAQ, Atmospheric Environment, 184, 146-155, https://doi.org/10.1016/j.atmosenv.2018.03.042, 2018.

Raatikainen, T., Vaattovaara, P., Tiitta, P., Miettinen, P., Rautiainen, J., Ehn, M., Kulmala, M., Laaksonen, A., and Worsnop, D. R.: Physicochemical properties and origin of organic groups detected in boreal forest using an aerosol mass spectrometer, Atmos. Chem. Phys., 10, 2063-2077, https://doi.org/10.5194/acp-10-2063-2010, 2010.

https://doi.org/10.5194/egusphere-2026-1023
Preprint. Discussion started: 16 March 2026

Ratcliff, M. A., Jr., Medley, E. E., and Simmonds, P. G.: Pyrolysis of amino acids. Mechanistic considerations, The Journal of Organic Chemistry, 39, 1481-1490, https://doi.org/10.1021/jo00924a007, 1974.
Riuttanen, L., Hulkkonen, M., Dal Maso, M., Junninen, H., and Kulmala, M.: Trajectory analysis of atmospheric transport of fine particles, SO 2, NO x and O 3 to the SMEAR II station in Finland in 1996–2008, Atmospheric Chemistry and Physics, 13, 2153-2164, https://doi.org/10.5194/acp-13-2153-2013, 2013.
Robinson, N. H., Hamilton, J. F., Allan, J. D., Langford, B., Oram, D. E., Chen, Q., Docherty, K., Farmer, D. K., Jimenez, J. L., Ward, M. W., Hewitt, C. N., Barley, M. H., Jenkin, M. E., Rickard, A. R., Martin, S. T., McFiggans, G., and Coe, H.: Evidence for a significant proportion of Secondary Organic Aerosol from isoprene above a maritime tropical forest, Atmos. Chem. Phys., 11, 1039-1050, https://doi.org/10.5194/acp-11-1039-2011, 2011.
Schauer, J. J., Rogge, W. F., Hildemann, L. M., Mazurek, M. A., Cass, G. R., and Simoneit, B. R. T.: Source apportionment of airborne particulate matter using organic compounds as tracers, Atmospheric Environment, 30, 3837-3855, https://doi.org/10.1016/1352-2310(96)00085-4, 1996.
Seinfeld, J. H. and Pandis, S. N.: Atmospheric chemistry and physics: from air pollution to climate change, John Wiley & Sons2016.
Simoneit, B. R. T.: Biomass burning — a review of organic tracers for smoke from incomplete combustion, Applied Geochemistry, 17, 129-162, https://doi.org/10.1016/S0883-2927(01)00061-0, 2002.
Simoneit, B. R. T., Rushdi, A. I., bin Abas, M. R., and Didyk, B. M.: Alkyl Amides and Nitriles as Novel Tracers for Biomass Burning, Environmental Science & Technology, 37, 16-21, https://doi.org/10.1021/es020811y, 2003.
Srivastava, D., Favez, O., Perraudin, E., Villenave, E., and Albinet, A.: Comparison of Measurement-Based Methodologies to Apportion Secondary Organic Carbon (SOC) in PM2.5: A Review of Recent Studies, Atmosphere, 9, 452, https://doi.org/10.3390/atmos9110452, 2018.
Stein, A. F., Draxler, R. R., Rolph, G. D., Stunder, B. J. B., Cohen, M. D., and Ngan, F.: NOAA's HYSPLIT atmospheric transport and dispersion modeling system, Bulletin of the American Meteorological Society, 96, 2059-2077, https://doi.org/10.1175/BAMS-D-14-00110.1, 2015.
Szidat, S., Jenk, T. M., Synal, H.-A., Kalberer, M., Wacker, L., Hajdas, I., Kasper-Giebl, A., and Baltensperger, U.: Contributions of fossil fuel, biomass-burning, and biogenic emissions to carbonaceous aerosols in Zurich as traced by 14C, Journal of Geophysical Research: Atmospheres, 111, https://doi.org/10.1029/2005JD006590, 2006.
Tarvainen, V., Hakola, H., Hellén, H., Bäck, J., Hari, P., and Kulmala, M.: Temperature and light dependence of the VOC emissions of Scots pine, Atmospheric Chemistry and Physics, 5, 989-998, https://doi.org/10.5194/acp-5-989-2005, 2005.
Ulbrich, I., Canagaratna, M., Zhang, Q., Worsnop, D., and Jimenez, J.: Interpretation of organic components from Positive Matrix Factorization of aerosol mass spectrometric data, Atmospheric Chemistry and Physics, 9, 2891-2918, https://doi.org/10.5194/acp-9-2891-2009, 2009a.
Ulbrich, I. M., Handschy, A., Lechner, M., and Jimenez, J. L.: AMS Spectral Database, University of Colorado Boulder [dataset], 2009b.
Varga, B., Kiss, G., Ganszky, I., Gelencsér, A., and Krivácsy, Z.: Isolation of water-soluble organic matter from atmospheric aerosol, Talanta, 55, 561-572, https://doi.org/10.1016/S0039-9140(01)00446-5, 2001.
Vogel, A. L., Äijälä, M., Corrigan, A. L., Junninen, H., Ehn, M., Petäjä, T., Worsnop, D. R., Kulmala, M., Russell, L. M., Williams, J., and Hoffmann, T.: In situ submicron organic aerosol characterization at a boreal forest research station during HUMPPA-COPEC 2010 using soft and hard ionization mass spectrometry, Atmos. Chem. Phys., 13, 10933-10950, https://doi.org/10.5194/acp-13-10933-2013, 2013.
Williams, J., Crowley, J., Fischer, H., Harder, H., Martinez, M., Petäjä, T., Rinne, J., Bäck, J., Boy, M., Dal Maso, M., Hakala, J., Kajos, M., Keronen, P., Rantala, P., Aalto, J., Aaltonen, H., Paatero, J., Vesala, T., Hakola, H., Levula, J., Pohja, T., Herrmann, F., Auld, J., Mesarchaki, E., Song, W., Yassaa, N., Nölscher, A., Johnson, A. M., Custer, T., Sinha, V., Thieser, J., Pouvesle, N., Taraborrelli, D., Tang, M. J., Bozem, H., Hosaynali-Beygi, Z., Axinte, R., Oswald, R., Novelli, A., Kubistin, D., Hens, K., Javed, U., Trawny, K., Breitenberger, C., Hidalgo, P. J., Ebben, C. J., Geiger, F. M., Corrigan, A. L., Russell, L. M., Ouwersloot, H. G., Vilà-Guerau de Arellano, J., Ganzeveld, L., Vogel, A., Beck, M., Bayerle, A., Kampf, C. J., Bertelmann, M., Köllner, F., Hoffmann, T., Valverde, J., González, D., Riekkola, M. L., Kulmala, M., and Lelieveld, J.: The summertime Boreal forest field measurement intensive (HUMPPA-COPEC-2010): an overview of meteorological and chemical influences, Atmos. Chem. Phys., 11, 10599-10618, https://doi.org/10.5194/acp-11-10599-2011, 2011.

https://doi.org/10.5194/egusphere-2026-1023
Preprint. Discussion started: 16 March 2026

Xu, L., Guo, H., Weber, R. J., and Ng, N. L.: Chemical Characterization of Water-Soluble Organic Aerosol in Contrasting Rural and Urban Environments in the Southeastern United States, Environmental Science & Technology, 51, 78-88, https://doi.org/10.1021/acs.est.6b05002, 2017.

Yan, C., Nie, W., Äijälä, M., Rissanen, M. P., Canagaratna, M. R., Massoli, P., Junninen, H., Jokinen, T., Sarnela, N., and Häme, S. A.: Source characterization of highly oxidized multifunctional compounds in a boreal forest environment using positive matrix factorization, Atmospheric Chemistry and Physics, 16, 12715-12731, https://doi.org/10.5194/acp-16-12715-2016, 2016.

Yasmeen, F., Szmigielski, R., Vermeylen, R., Gómez-González, Y., Surratt, J. D., Chan, A. W. H., Seinfeld, J. H., Maenhaut, W., and Claeys, M.: Mass spectrometric characterization of isomeric terpenoic acids from the oxidation of α-pinene, β-pinene, d-limonene, and Δ3-carene in fine forest aerosol, Journal of Mass Spectrometry, 46, 425-442, https://doi.org/10.1002/jms.1911, 2011.

Yin, J., Cumberland, S. A., Harrison, R. M., Allan, J., Young, D. E., Williams, P. I., and Coe, H.: Receptor modelling of fine particles in southern England using CMB including comparison with AMS-PMF factors, Atmos. Chem. Phys., 15, 2139-2158, https://doi.org/10.5194/acp-15-2139-2015, 2015.

Ylivinkka, I., Di Natale, C., Mikkelsen, M. K., Nissinen, A., Pennacchio, L., Strömberg, J., Saranko, O., Utriainen, L., Valiati, R., and Aalto, J.: Intervention of pollution episodes from nearby sawmills to ecosystem-atmosphere interactions studied in a boreal forest at SMEAR II, https://doi.org/10.60910/ber2025.727e-sw95, 2025.

Yttri, K. E., Simpson, D., Nøjgaard, J. K., Kristensen, K., Genberg, J., Stenström, K., Swietlicki, E., Hillamo, R., Aurela, M., Bauer, H., Offenberg, J. H., Jaoui, M., Dye, C., Eckhardt, S., Burkhart, J. F., Stohl, A., and Glasius, M.: Source apportionment of the summer time carbonaceous aerosol at Nordic rural background sites, Atmos. Chem. Phys., 11, 13339-13357, 10.5194/acp-11-13339-2011, 2011.

Zhang, Q., Jimenez, J. L., Canagaratna, M. R., Ulbrich, I. M., Ng, N. L., Worsnop, D. R., and Sun, Y.: Understanding atmospheric organic aerosols via factor analysis of aerosol mass spectrometry: a review, Analytical and Bioanalytical Chemistry, 401, 3045-3067, https://doi.org/10.1007/s00216-011-5355-y, 2011.

Zhang, T., Shen, Z., Huang, S., Lei, Y., Zeng, Y., Sun, J., Zhang, Q., Ho, S. S. H., Xu, H., and Cao, J.: Optical properties, molecular characterizations, and oxidative potentials of different polarity levels of water-soluble organic matters in winter PM2.5 in six China's megacities, Science of The Total Environment, 853, 158600, https://doi.org/10.1016/j.scitotenv.2022.158600, 2022.

Zhang, X., Hecobian, A., Zheng, M., Frank, N. H., and Weber, R. J.: Biomass burning impact on PM_{2.5} over the southeastern US during 2007: integrating chemically speciated FRM filter measurements, MODIS fire counts and PMF analysis, Atmos. Chem. Phys., 10, 6839-6853, https://doi.org/10.5194/acp-10-6839-2010, 2010.

Zhang, Y., Heikkinen, L., Äijälä, M., Peräkylä, O., Graeffe, F., Mickwitz, V., Zhao, J., Daellenbach, K., Sueper, D., Worsnop, D., Riva, M., and Ehn, M.: Enhanced Aerosol Source Identification by Utilizing High Molecular Weight Signals in Aerosol Mass Spectra, ACS ES&T Air, 1, 502-510, https://doi.org/10.1021/acsestair.3c00102, 2024.

Zheng, Y., Horowitz, L. W., Menzel, R., Paynter, D. J., Naik, V., Li, J., and Mao, J.: Anthropogenic amplification of biogenic secondary organic aerosol production, Atmos. Chem. Phys., 23, 8993-9007, https://doi.org/10.5194/acp-23-8993-2023, 2023.

Zhou, R., Chen, Q., Chen, J., Ren, L., Deng, Y., Vodicka, P., Deshmukh, D. K., Kawamura, K., Fu, P., and Mochida, M.: Distinctive Sources Govern Organic Aerosol Fractions with Different Degrees of Oxygenation in the Urban Atmosphere, Environ Sci Technol, 55, 4494-4503, https://doi.org/10.1021/acs.est.0c08604, 2021.